

Wave Energy Deployments Physical Impact Guidelines

Prepared by Kathleen McInnes, Mark Hemer, Julian O'Grady, Ron Hoeke, Stephanie Contardo

February 2018



CSIRO Oceans and Atmosphere Business Unit

<https://www.csiro.au/en/Research/OandA>

Authors

Kathy McInnes

Mark Hemer

Julian O’Grady

Ron Hoeke

Stephanie Contardo

Citation

McInnes KL, Hemer MA, O’Grady JG, Hoeke, RK, Contardo, S (2018) Wave Energy Deployments Physical Impact Guidelines. Report for ARENA CSIRO, Australia. 78pp.

Copyright

© Commonwealth Scientific and Industrial Research Organisation 20XX. To the extent permitted by law, all rights are reserved and no part of this publication covered by copyright may be reproduced or copied in any form or by any means except with the written permission of CSIRO.

Important disclaimer

CSIRO advises that the information contained in this publication comprises general statements based on scientific research. The reader is advised and needs to be aware that such information may be incomplete or unable to be used in any specific situation. No reliance or actions must therefore be made on that information without seeking prior expert professional, scientific and technical advice. To the extent permitted by law, CSIRO (including its employees and consultants) excludes all liability to any person for any consequences, including but not limited to all losses, damages, costs, expenses and any other compensation, arising directly or indirectly from using this publication (in part or in whole) and any information or material contained in it.

CSIRO is committed to providing web accessible content wherever possible. If you are having difficulties with accessing this document please contact csiroenquiries@csiro.au.

Contents

Abbreviations and Glossary.....	4
Executive Summary	5
1 Introduction	9
1.1 Background	9
1.2 Scope of this Document.....	10
2 State of the Science.....	12
3 Simulations to support guidelines development	16
3.1 Wave climate	16
3.2 Idealised Nearshore Morphology	17
3.3 WEC device types.....	19
3.4 WEC array configurations	19
3.5 Numerical Simulation Model	24
3.6 Analysis Methods and Defining Impact Zones.....	26
4 Wave array impact zone analysis.....	28
4.1 Wave climate and nearshore profile	28
4.2 WEC array configuration.....	31
4.3 Semi-empirical equations for quantifying down-wave impact.	35
5 Summary and Next Steps	44
References	48
Appendix A: Australian Wave Energy Resource and Developments.....	51
Appendix B: Planning and Legislative Considerations.....	55
Appendix C: Characterising Wave Climates using MDA.....	57
Appendix D: Nearshore Morphology.....	60
Appendix E: SNL-SWAN Model Configuration.....	61
Appendix F: Impact zone analysis.....	62

Appendix G: Empirical Equation Parameters. 64

Appendix H: Supplementary plots..... 75

Abbreviations and Glossary

AWavEA	Australian Wave Energy Atlas Project
ADCP	Acoustic Doppler Current Profiler
CETO5	Wave Energy Converter developed by Carnegie Pty Ltd rated at 240 kW
CSIRO	Commonwealth Scientific and Industrial Research Organization
PPA	Power Purchase Agreement
REC	Renewable Energy Certificate
SNL-SWAN	Version of SWAN developed by Sandia National Laboratories to account for the wave frequency and wave height dependent transmission (absorption) of a WEC
SWAN	Simulating WAVes Nearshore – Spectral wave model
WEC	Wave Energy Converter
Xbeach	Two-dimensional model for wave propagation, sediment transport and morphological changes of the nearshore area, beaches, dunes and back barrier during storms.

Executive Summary

Australia's wave energy resource has been assessed as being arguably the largest in the world, thereby providing a potential future renewable energy resource to Australia's renewable energy portfolio. The past decade has seen several wave energy prototypes trialled in the Australian ocean environment. However, the wave energy industry globally is in its infancy and faces a range of barriers to becoming financially viable. One challenge is the uncertainty of the consenting processes, particularly in regards to the environmental impact assessment for the development and operation of ocean energy facilities.

To support the development of the wave energy industry in Australia, this document addresses the limited evidence base and methodology for assessing impacts of wave energy extraction on the marine and coastal environment. In particular, this document provides best practice guidance on assessing the influence of arrays of Wave Energy Converters (WECs) on the hydrodynamic attributes of the surrounding ocean. These guidelines have been developed as part of the ARENA and CSIRO-funded Australian Wave Energy Atlas Project (AWavEA). A wave energy project cycle typically consists of four stages (Appendix B): Preliminary evaluation; Feasibility study; Project design; and Implementation and operation. The guidelines presented in this report aim to support preliminary assessments of the suitability of a proposed site to deployment of wave energy converters.

The development of the guidelines combines information obtained from a large suite of idealised numerical modelling experiments, using a model configuration which has been calibrated and validated with observations from a dedicated field experiment – the Garden Island field study.

The Garden Island field study carried out as part of the AWavEA project enabled the direct measurement of the wave energy extracted from a deployed wave energy converter and the assessment of SNL-SWANs suitability for use in the development of the guidelines. The focus of the guidelines is on providing preliminary estimates of the extent of impact in the mid-to-far field (away from the immediate proximity of the WEC array) for which SNL-SWAN was found to be suitable. Accompanying scaled physical experiments have been carried out at the facilities of the Australian Maritime College, University of Tasmania. These experiments resolve changes to the wave field induced by the presence of WECs, which occur in the near-field (immediate proximity of the WECs) and are difficult to

measure in the field environment (e.g., diffraction, the radiated wave field). The tank experiments will aid development of future models which can account for the full range of processes poorly captured by the phase-averaged SNL-SWAN model (i.e., near-field effects), but have not been used to underpin the guidelines developed here.

Simulations by computational wave models provide a cost-effective approach to investigating the effect of wave energy devices on the surrounding ocean wave field, provided they are suitably calibrated/validated with high-quality observations from scale experiments (e.g. laboratory test basins) or full scale deployments. A validated numerical model will allow exploration of a much larger number of scenarios than be achieved in an observational setting. Different computational modelling approaches are available ranging from those capable of representing the interactions between individual devices to the less computationally expensive phase-averaged approaches that parameterise the attenuation effects of wave devices. The phase-averaged wave model SNL-SWAN, is able to represent the wave field attenuation produced by WECs using frequency-dependent transmission (absorption) coefficients by incorporating wave energy device “power matrices” that represent the power extracted by specific wave energy devices. However the model has limitations, particularly in assessing near-field effects in the immediate vicinity of the WECs, as it is not designed to account for key processes in this zone (i.e., diffraction, the radiated wave from the WEC, and thus WEC-WEC interactions).

A series of idealised simulations using SNL-SWAN of WEC array installations was performed in order to underpin the development of the guidelines. Factors considered were different device types (four in total plus a ‘no device’ baseline simulation) with two different array sizes (3 MW and 20 MW) and two configurations (a two-row and a square array). These configurations were modelled under the wave climate conditions of four locations around Australia (Perth, Albany, Port Fairy and Sydney), each of which have good wave energy resource, proximity to population centres and electrical transmission infrastructure. Idealised straight and parallel nearshore morphology was assumed with two different bathymetric slopes, a steep and a gentle equilibrium profile, with the WEC array in 25 m depth at 2 and 4 km offshore respectively. To reduce the number of simulations under the different wave conditions of each location, the 34 years of hourly wave climate data, comprising about 300,000 data points, was generalised to about 500 representative sea states with associated probabilities of occurrence at each location. Together, these considerations amounted to 68,000 simulations (4 locations × 2 slopes × (1 baseline + (4 devices × 2 array sizes × 2 array configurations)) × 500 wave conditions).

The impact of the WEC array is determined by changes in wave field parameters on the shoreward side (i.e. down-wave) of the WEC array. The parameters considered are the 50th, 75th and 90th percentile values of;

1. Significant wave height (H_s) climate – representing an easily understandable indicator of change and also related to other wave field parameters, such as wave orbital velocity.
2. Wave power (CgE) - indicating impacts on the energy resource.
3. Maximum near-bottom orbital velocity (U_o) - indicating changes to seabed mobility transport
4. Dissipation due to depth-induced breaking (D_{surf}) – indicating energy dissipation due to surf breaking (in W/m^2) near the shoreline.

The results are generalized by developing empirical equations that represent zones of impact in terms of;

1. Area of impact.
2. Distance of impact in the cross-shore (shore-perpendicular) direction from the array towards the shoreline
3. Distance of impact in the longshore direction (shore-parallel) in the far field, which is defined as the region within 1 km of the coastline for the gentle profile, and within 500 m of the coastline for the steep profile, at approximately the 10 m depth contour.

The zones of impact are applied to wave field parameters of H_s , CgE , U_o and D_{surf} down-wave of the array as a function of the input variables including wave parameter, change in wave parameter and power output of the array. Look-up tables are provided for the coefficients to apply the equation to different types of impact assessment and the estimated error in the empirical equation. Hypothetical examples are provided to illustrate the use of the equations.

In addition to developing empirical equations for estimating the impacts of arrays of wave energy devices, analysis of the simulations yielded some general findings about the impacts of WEC arrays on the surrounding wave field as summarised below;

- 1) The impact of WEC arrays containing many devices with lower power ratings will have less intense (point-source) impact on the near to mid field than fewer devices that extract larger amounts of power. Maximising power extraction for a single device will therefore have a larger impact on the near- to mid-field environment.
- 2) WEC arrays deployed closer to the coast have increased impact in the breaking zone. Simulations show that significant changes in the radiation stress force associated with the predicted energy

reductions could be expected. If the cross-shore impacted distance in the wave field (e.g., in H_s) intersects the wave breaking depth, the equilibrium state of the coastal zone will likely be disturbed leading to changes in coastal properties (e.g., shoreline position). This may be considered a positive or negative effect – for example, in some cases, a WEC array might be deployed as a coastal management solution. **The recommendation from this study is if the estimated cross-shore impact distance intersects the 10-m depth contour, a more rigorous impacts study is required for the coastal zone.**

- 3) A directional wave climate that is more widely distributed (e.g. Sydney) will have a less focussed impact on the coastline than a narrow directional wave climate.

It is noted that the limitations of the SNL-SWAN wave model together with the use of idealised simulations to develop the generic tools detailed in these guidelines necessarily means that their application is limited to providing only preliminary assessments and broad guidance of the impact of wave arrays. Factors such as the wave environment, the wave energy devices, their arrangement in arrays and the total power output have been considered in developing a quantitative impact equation. Given the idealised nature of the experiments undertaken and the generalisation of the findings into a single impact equation, the guidance provided should be considered to be approximate at best, potentially providing the broad requirements in the specific coastal environment under consideration. For example, these preliminary assessments may inform the design of more detailed modelling assessments that account for the specific attributes of the devices and the local environment under investigation. The assessments may also be used to inform the monitoring of the identified impacts by providing guidance on the most suitable locations for deployment of instrumentation.

1 Introduction

1.1 Background

In a world challenged by increasing energy demands and the need to reduce greenhouse gas emissions in the face of climate change, energy derived from ocean waves has the potential to contribute to a future energy portfolio that is increasingly reliant on renewable energy sources. The ocean possesses a largely untapped renewable energy resource with the potential to provide clean electricity to coastal communities and cities. Moreover, Australia has been assessed as having arguably the largest wave energy resource of any country (Hemer et al., 2016; see also Appendix A.1), and is therefore well positioned to benefit from development of the sector.

Globally the ocean renewable energy sector is in its infancy and it faces various barriers that must be overcome to become financially viable. One of the biggest challenges facing the emergent ocean energy industry today is uncertainty in relation to consenting processes under domestic legal systems (Simas et al., 2015; O'Hagan, 2016). One of the most significant regulatory challenges which arises is assessment of the environmental impact associated with the development and operation of ocean energy facilities. Single devices are unlikely to have adverse environmental impacts (Copping et al., 2016). However large arrays of Wave Energy Converters (WECs), which will be needed if wave energy is to make a meaningful contribution to the future energy mix, may cause a range of impacts on the ocean environment. Potential environmental effects include changes to environmental flows around devices, the effect of noise or electro-magnetic radiation on marine species and changes in benthic habitats and reefing patterns, although, the evidence base to assess such impacts remains low (Copping et al., 2016).

The purpose of this document is to present best practice guidance on the influence of arrays of Wave Energy Converters (WECs) on the hydrodynamic attributes of the surrounding ocean, to support preliminary evaluation of the suitability of a site to the deployment of a WEC array. These guidelines have been developed as part of the ARENA and CSIRO-funded Australian Wave Energy Atlas Project (AWavEA), which was initiated to address knowledge gaps presently faced by the industry in Australia. These guidelines specifically address the limited evidence base and methodology for assessing impacts of wave energy extraction on the marine and coastal environment. In particular, guidance is provided on the methodology and criteria used to establish zones of impact defined in terms of changes in local wave

energy spectra downstream of a wave energy conversion site. The development of the guidelines combines information obtained from field observations together with numerical modelling.

1.2 Scope of this Document

Although the marine renewable energy sector is not yet mature, a diverse range of WECs have been designed to date that utilise different physical principals for wave energy extraction. A number of these designs have been trialled in Australian waters. The experience and lessons learnt from these projects serve to benefit the community as a whole. A brief summary of the different device designs and trials that have been undertaken across Australia to date is provided in Appendix A.

Prospective marine energy developers need to seek approvals to undertake marine energy projects on Crown land. This document provides information on the regulatory framework operating across Australia that developers are required to consider in the planning and design phase of wave energy projects for seeking permits for WEC projects. This information is presented in Appendix B.

The primary focus of this document is to present guidance on evaluating the impact of WEC's on the physical wave field in the ocean environment down-wave of a WEC array. The development of a wave model for this purpose has been supported by data from an observational field program together with laboratory results. The field observations and laboratory experiments have been used to calibrate a numerical model, which is then used to undertake idealised simulations of a number of WEC array installations in different physical environments. The data from these numerical experiments underpin the development of a set of tools and guidelines material that can be applied to establish broad estimates of the zone of impact on the local wave energy spectra down-wave of a WEC array.

The report does not aim to comprehensively address the potential environmental effects of arrays of WECs. Changes in the adjacent hydrodynamics due to the presence of WECs may influence ecological communities. This is not addressed by the report, nor are the potential effects of noise or electromagnetic radiation.

2 State of the Science

An important component of the site selection process for wave energy developments is an assessment of the impact of an array of wave energy converters on the local wave climate. Such assessments help inform decisions on the optimal layout of WEC arrays to maximise power output and also the likely impacts the development will have on the surrounding environment (O'Boyle et al., 2017). The growing interest in wave renewable energy over the past two decades has seen an increase in studies that assess the potential impact of wave energy devices. The approaches used have typically relied on numerical wave modelling (simulation) and on direct observations, either in physical tanks (laboratory test basins) or in open ocean settings.

Numerical simulation provides the benefit of enabling simulations of hypothetical wave arrays in different coastal settings to explore a large number of potential scenarios which cannot be investigated in an observational setting. An important step is to ensure the model is sufficiently calibrated and validated using observational data from either scale experiments (e.g. laboratory test basins) or full scale deployments. Folley et al. (2012) reviews the different numerical wave models (including Boussinesq, mild-slope and spectral approaches), which have been used to investigate changes in the adjacent wave field, but have no ability to determine device hydrodynamics. To account for device hydrodynamics, Potential Flow Models or Computational Fluid Dynamics (CFD) models have historically been used, although recent development has seen application of the non-hydrostatic wave-flow model SWASH to capture these effects (Rijnsdorp et al., 2017). Whilst these models may provide enhanced representation of interactions, they come at significantly greater computational expense, and are specific to the device which has been configured. Given WEC design is still an open field, with no convergence on device design, there is an advantage in being able to generalise the parameterisation of attenuation effects on the basis of WEC power output, irrespective of design, as has been introduced into the phase-averaged model SNL-SWAN. The challenge to date for all models has been the limited observations available to validate these numerical approaches.

Several studies have sought to measure the attenuation of the wave field surrounding scaled WEC arrays deployed in laboratory test basins. In such studies, the wave field downstream of the scaled devices in a laboratory tank, is measured using distributed resistive wave gauges (Alexandre et al., 2009, Haller et al., 2011, McNatt, 2012, O'Boyle et al., 2017), or new video-grammetry techniques easily employed in the laboratory settings (Black, 2014, Winship et al., in prep).

The increase in number of wave energy demonstration projects being deployed in the open ocean is providing opportunity to undertake direct observations of the impact of the WECs on the surrounding wave field in an open ocean environment, which helps validate and further refine the modelling approaches (e.g. Ashton et al., 2013; Contardo et al., 2017). Ashton et al. (2013) demonstrated the high degree of spatial variability in wave field across a proposed full-scale wave energy test site. This highlights the requirement for accurate evaluation of physical processes at the test site since differences in the wave climate between the point of measurement and the location at which a device is to be situated will affect the resource assessment and device performance. Contardo et al. (2017) analysed wave measurements from the up-wave and down-wave sides of several operational WECs deployed in 23 m water depth, 4 km offshore from Garden Island in Western Australia. These observations indicated a small amount of statistically significant wave energy absorption at discrete frequencies due to the WEC(s).

Results from a calibrated SNL-SWAN wave model (Ruehl et al., 2015) incorporating frequency-dependent transmission (absorption) coefficients from a “power matrix” based on the power output extracted by the WEC highlighted that such industry standard device power matrices cannot fully describe the actual power removed from the natural wave field at discrete wave frequencies, because:

- 1) The power matrix is based on the absorbing (blocking) of bulk/integrated wave climate statistics (H_s, T_p), which cannot describe the discrete wave frequency transmission (blocking) that was measured in the field.
- 2) The power matrix does not account for wave energy that is blocked/removed by the device but not turned into power output, e.g. waves breaking on the device damping the motion and power output.
- 3) Measurement of waves down-wave of a WEC obstacle in a random wave field (and sufficiently far away not to be measuring the direct motion of the WEC) will be influenced by waves from oblique angles around the device, so a numerical model is required to estimate this additional component in determining the transmission in an operational environment.

Despite these factors, the Garden Island study found both methods of discrete frequency transmission and transmission of the bulk wave parameters (obstacle case 1), resulted in very similar statistics when considering the overall transmission of bulk/integrated wave climate statistics.

An assessment of the effect of WEC arrays on the local wave field is necessary to inform decisions on the layout of wave arrays for optimisation of the power output and also for assessing and minimising the

environmental impact of such developments or understanding their potential for coastal protection. A number of studies have addressed these issues.

The potential dual benefits of wave energy production and coastal protection from WECs has been investigated by Abanades et al., (2015a, b) using SWAN and Xbeach. They find the distance of the wave array to the coast is a key determining factor in the effectiveness of a WEC array for coastal protection. Numerical modelling of a 2-row configuration of 11 overtopping WECs located at distances of 2, 4 and 6 km from the 10 m reference depth contour in water depths varying from 25 to 35 m yielded average reductions in significant wave height of 25%, 15% and 9% respectively. Changes in bed level arising from the reduced wave energy were most apparent at the beach face for the WEC array closest to shore, where erosion (measured as a reduction in elevation of the beach) was reduced by up to 1.5 m compared to the no-WEC case. There was also an associated change from wave-dominated to tide-dominated morphological characteristics when the WEC array was closest to shore compared to the no-WEC case. However, the reduction of wave energy resource from the site furthest offshore to the site closest inshore was about 10% indicating there is a trade-off between the coastal protection benefits and energy production benefits of WECs in selecting the location for WEC deployment.

In a modelling study to explore the impact of a WEC test site Chang et al, (2012) modelled the impact of three WECs on the wave climate in Kaneohe Bay, Hawaii. The devices were conservatively assumed to completely absorb the incident wave energy and were found to reduce H_s and orbital velocities at the 5 and 10 m depth contours by around 6% leading to the conclusion that the impact of the WECs at the test site were likely to have a negligible impact on the environment. A subsequent study in Monterey (Chang et al, 2014) used the same modelling approach to examine the impact on wave fields of two commonly proposed configurations for point-absorber WECs. The first was a honeycomb configuration, commonly proposed for point absorbers, consisting of 10 WECs in 50 m of water oriented such that the broadest array dimension was perpendicular to the incident wave angle. A second set of experiments involved a diamond-shaped configuration comprising 10, 50, 100 and 200 WECs. The impact on the wave field of different WEC separations ranging from 2.5 to 10 times the WEC diameter was also investigated. The closer spacing of WEC devices (e.g. 2.5x) resulted in a larger decrease in wave energy propagation near the array compared to larger spaced arrays (5x or 10x spacing); The far-field effect of a closer-spaced array on the wave conditions was not as significant as larger-spaced arrays. The transmission coefficient was shown to generate the largest sensitivity in honeycomb WEC array simulations. The diamond-shaped WEC arrays were most sensitive to the variation in the parameters in terms of effect on wave heights.

In Australia, Flocard and Hoeke (2017) used the SNL-SWAN model to assess the impact on wave height and bottom orbital velocity of bottom-fixed, rotating WECs at East Beach, Port Fairy in Victoria. The WECs were configured in arrays consisting of 15, 30 or 60 devices located between 1.6 and 2.4 km from the shore in water depths ranging from 17 to 26 m. Incident wave conditions consisted of three different storm events with average recurrence intervals of 0.5 to 1 years. Results indicated that an array of 30 to 60 WECs, located about 1.5 km from the shore could be associated with a 30% nearshore reduction of wave height during 0.5 to 1 year ARI storms, which likely would be associated with a reduction of the erosion on the upper beach face.

While WEC arrays have the ability to reduce hydrokinetic energy from the nearshore region with the potential benefit of reducing coastal erosion, there may also be ecological implications owing to the potential effect of reduced hydrokinetic energy. The potential effects of WEC arrays on benthic habitats, by shifting the equilibrium energy levels to which the ecological system may be adapted to, is often identified as a possible negative effect of WEC array deployment. Studies to date suggest it is unlikely that wave arrays will cause substantial alteration to benthic habitats, particularly when compared to other human activities (e.g., commercial trawl fisheries; Witt et al., 2011), although this is based on little quantitative data. Other systems also need further consideration - For example, a reduction in wave energy acting on the shoreline would reduce the height of the effective wetting level of the sea, thus reducing the area of habitat available for intertidal marine organisms (Shields et al., 2011).

3 Simulations to support guidelines development

This section describes a series of idealised simulations of WEC array installations performed in order to underpin the development of the guidelines. These idealised simulations are necessary since the various studies reported in the last section are site-specific and a more generalised approach is needed. The simulations complement the measurements and modelling in the Garden Island field study (Contardo et al., 2017) and the scaled physical experiments carried out in the laboratory (Winship et al., in prep) as part of the Project; they investigate the effect of different WEC array configurations, different device types and different (simplified) physical settings. These simulations are not intended to be comprehensive, nor could they be: the number of potential permutations of array/device configurations and important local environmental (physical, geological, ecological) and human (societal, economic, infrastructure) attributes at potential installation sites could be nearly infinite. However, these simulations attempt to broadly capture physical impacts that are nationally relevant for Australia by making a number of simplifying assumptions and therefore reducing the number of simulations and subsequent analysis to a tractable size. These simplifying assumptions include restricting the total number of WEC device types, WEC array configurations and wave climates considered and performing the simulations at two different idealised nearshore morphologies; four different output variables were considered for subsequent analyses. Despite these simplifying assumptions, the total number of simulations performed is 68000. The following sub-sections describe these simplifying assumptions, the numerical model selected to perform the simulations and the analyses in brief - more complete technical descriptions can be found in the Appendices.

3.1 Wave climate

Wave information from four locations located offshore from Perth, Albany, Port Fairy and Sydney, was extracted from the CAWCR wave hindcast (Durrant et al. 2014). While they do not represent all of Australia's varied wave climates, these locations represent a range of possible conditions in areas with good wave energy resource and/or proximity to population centres/electrical transmission infrastructure (Hemer et al., 2016). Characteristics of these wave climates are presented as wave roses in Figure 1.

For each location, the 34 years of hourly wave (sea-state) statistics amounted to approximately 300,000 data points. To reduce this to a tractable number, an algorithm was applied to the entire set of data points to select a subset of which best statistically represented the data as a whole (similar to that described by Camus et al., 2011, see Appendix A for details). This resulted in 500 individual sea states, with associated

probabilities of occurrence, at each location. These data were used to provide forcing at the offshore boundary of the nearshore wave model used for the simulations described in Section 5.5.

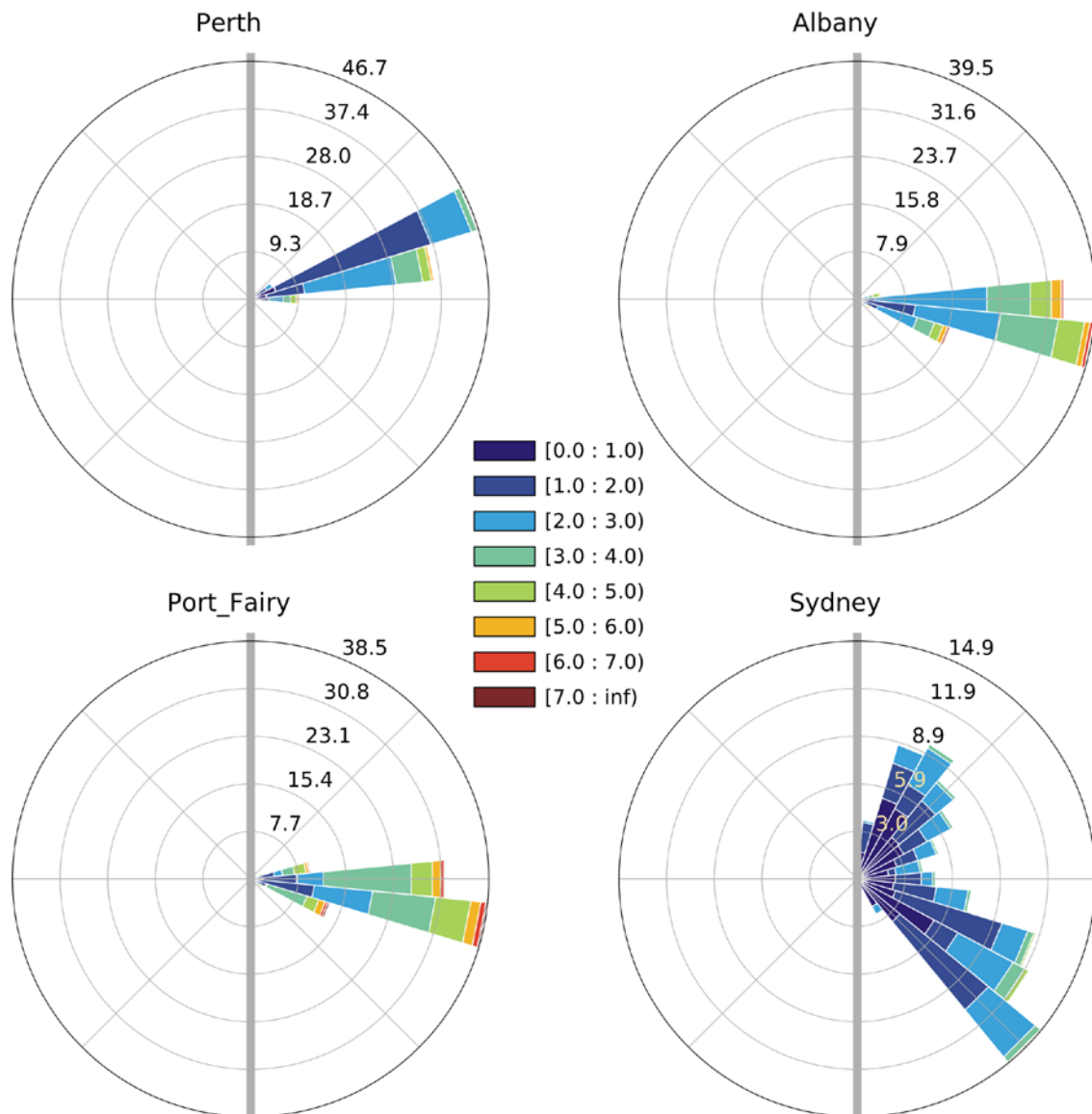


Figure 1: Wave roses showing the wave climate for the four sites considered. The coastline direction is shown by the solid grey line with ocean to the right. Wave directions use nautical convention and hence indicate the direction from which the waves approach the coast. Travelling clockwise long the Australian coastline, the design coastline bearing is 222° for Sydney, 315° for Port Fairy, 296° for Albany and 353° for Perth.

3.2 Idealised Nearshore Morphology

Nearshore wave propagation and dissipation is highly dependent on littoral zone morphology, e.g. offshore bathymetry and coastal headlands may focus waves in some areas more than others, offshore reefs may shelter some beaches and nearshore zones more than others, and so on. These in turn, largely control other processes/characteristics, e.g. erosion and accretion of shorelines and the distribution of benthic habitats. Generalising this nearshore morphology in a meaningful way, applicable to large swaths of the

Australian coastline, would be an enormous research task, even without considering the potential role of WEC arrays on nearshore wave propagation and dissipation. Therefore a simple approach is opted for here: the idealised nearshore morphology is assumed to consist of alongshore uniform (straight and parallel) bathymetric contours, a simplification often used in conceptual or idealised coastal modelling. Based on the average distance between the shoreline and the 25m depth contour around Australia, two nearshore profiles were constructed: 1) a relatively steep profile, tending to be more representative of Australia’s east coast, and 2) a gentle profile, tending to be more representative of an Australian south or west coast profile. Both of these profiles are assumed to be “equilibrium” profiles consisting of sandy substrates. For more detailed information on methods used to construct the nearshore morphologies and associated simulation domains, see Appendix B. These simplifying assumptions were used to construct two simulation domains (one for each profile type): both are 12 km wide (in the shore-parallel direction) and 6 km across (in the shore-perpendicular direction), with water depths ranging from 0 to at least 40 m deep. WEC arrays were positioned to be centred in the domain in the shore-parallel direction and on the 25 m deep contour in the shore-perpendicular direction. 25 m was chosen as being a representative target depth at which the four chosen WEC designs would be deployed. Figure 2 illustrates the two simulation domain types with an example WEC array situated within them.

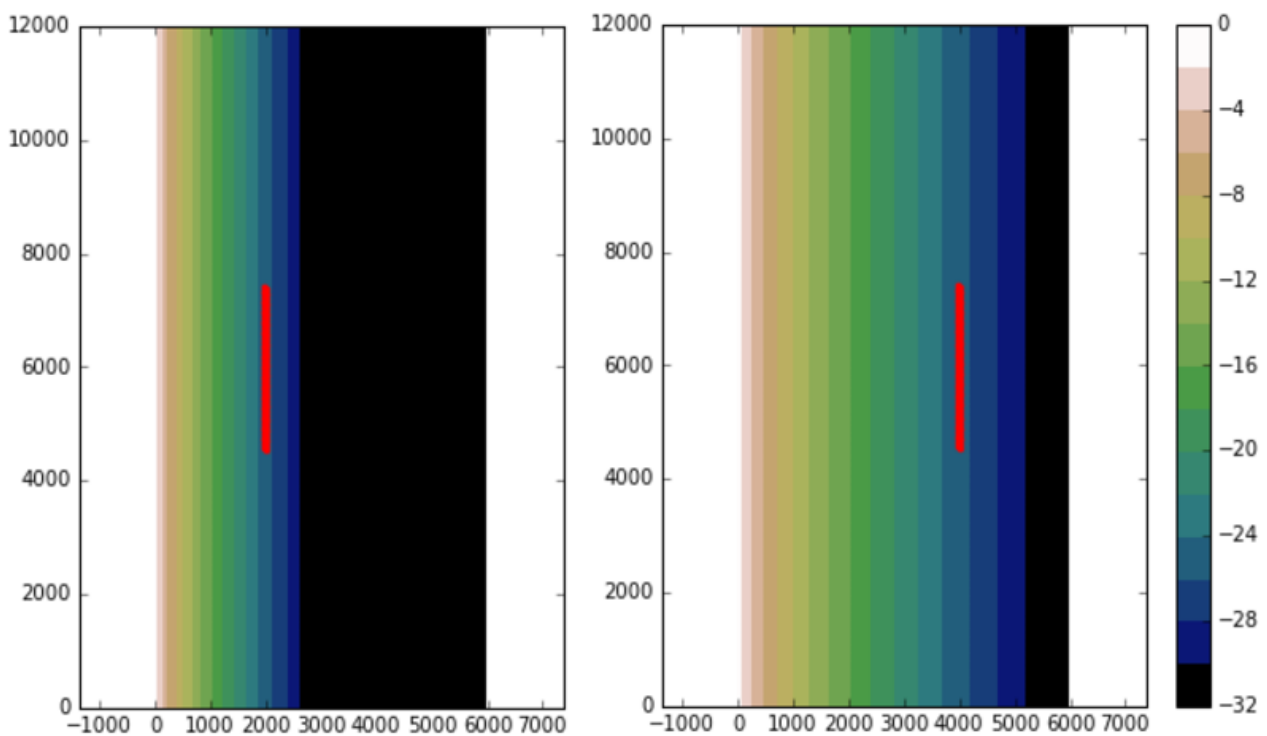


Figure 2: The two types of simulation domains with depths (bathymetry) indicated in colours. The steeper bathymetric profile on the left is more typical of the east coast and the gentler (more gradual) bathymetric profile on the right is more typical of west and south coasts. The red lines in both domains indicates the positioning of a two-row array of 48 WECs, as an example of the WEC array positioning used in the simulations.

3.3 WEC device types

Four contrasting WEC designs were chosen to represent the range of WECs that might be deployed off the Australian coast. The WECs represent differing device types, which utilise different physical principals for wave energy extraction; the nominal capacities of individual devices range from 200 kW to 3 MW and have performance metrics available in the public domain. The performance metric is based on the respective published power matrices derived from Babarit et al. (2011) and Flocard et al. (2012). While a selection of devices were chosen in order to explore the sample space associated with different devices, it should be noted that the four devices tested are similar in that they target resource offshore. Devices that operate in the breaking zone – for example operating on the principal of the submerged pressure differential – will be poorly represented by these experiments. Tables 3 briefly describes the devices selected for assessment.

Table 1 Description of WECs selected for assessment in this study.

WEC Name	Description	Nominal (Nameplate) Capacity (MW)
Bref-SHB	Bottom-referenced submerged heave buoy	0.209
F-OWC	Floating oscillating water column	2.880
B-OF	Bottom fixed oscillating flap	3.332
P-PA	Pitching point absorber	0.457

3.4 WEC array configurations

The different array configurations are characterised by array size, in terms of energy output, and array type, based on the physical layout of the devices. Two array sizes are considered: a 3 MW and 20 MW; and two array types are considered: a two row configuration in which the WECs within each row are staggered with respect to the other row; and a multi-staggered, multi-row configuration making up a square array. This results in a total of four array configurations: 3 MW and 20 MW size arrays of either a two-row or square type. These four array configurations are not intended to represent an optimisation for the four WEC devices considered or for particular wave climates, rather they are designed simply to provide a range of array configurations with which to (at least partially) explore possible parameter space and subsequent environmental impacts.

The (nameplate) nominal capacity was used to select the number of WECs required for the small 3 MW and large 20 MW arrays. The nominal capacity is the maximum output value in the device power-output matrix (listed in Table 3). The array configurations for each WEC device type are listed in Table 4.

Table 4 Array configurations. The ‘x’ symbol represents multiple rows of WECs, e.g. 8x2 is two rows of eight WECs.

WEC Name	Two Rows (small) 3 MW	Two Rows (large) 20 MW	Small Square 3 MW	Large Square 20 MW
Bref-SHB	8x2	48x2	4x4	10x9+6
F-OWC	1x1	4+3	1x1	3x2+1
B-OF	1x1	3x2	1x1	3x2
P-PA	4+3	22x2	3x2+1	7x6+2

Typical spacing between devices, especially between front and back row for optimal array setup is half a wave length of the peak period related to the WEC maximum power output (T_{p0}). The spacing of WEC devices is important for array and wave field interactions, such as wave focusing by wave diffraction and device resonance, which can improve/optimize WEC array power output. As the SNL-SWAN model cannot fully model these phase-resolved wave processes (diffraction and resonance), the output should not be sensitive to WEC spacing and so it is not a critical aspect of the design of these experiments.

The typical wave length of the T_{p0} waves in 25m of water ranges from 74 to 166 m for the devices considered, which averages out to 120m, therefore the WEC spacing in the model experiments is designed to be half this value, i.e. 60m (see Table C.1).

Table 5 WEC device wave lengths at maximum output and idealised spacing.

WEC Name	Device width (m)	T_{p0} (s)	Wavelength of nameplate output T_{p0} at 25 m depth	Ideal spacing
Bref-SHB	7	7	74	37
F-OWC	24	11	148	74
B-OF	26	12	166	83
P-PA	6	8	93	46.5
Average	15.75	9.5	120.25	60.125

Each of the four devices considered have specific power matrices, which will be associated with a specific amount of power absorbed from the wave field and associated attenuation effects. The width-normalised power absorbed by the device is described as:

$$\mathbf{P}_{absorbed}(\mathbf{H}_s, \mathbf{T}_p) = \frac{1}{w} [\mathbf{P}_{out}(\mathbf{H}_s, \mathbf{T}_p) + \mathbf{P}_{eff}(\mathbf{H}_s, \mathbf{T}_p)], \quad (1)$$

where \mathbf{P}_{out} is the device total power output matrix (electrical or mechanical) supplied by the operator, \mathbf{P}_{eff} is the transmission efficiency of the waves to output, $\mathbf{P}_{absorbed}$ is the width-normalised power absorption matrix of the wave field and w is the width of the device (Table 5). For simplicity \mathbf{P}_{eff} is set to zero. The transmission of the wave power is then described as:

$$K_t^2(\mathbf{H}_s, \mathbf{T}_p) = \mathbf{1} - \left(\frac{w}{l}\right) \frac{\mathbf{P}_{absorbed}(\mathbf{H}_s, \mathbf{T}_p)}{\mathbf{P}_{incident}(\mathbf{H}_s, \mathbf{T}_p)}, \quad (2)$$

where K_t^2 is the transmission factor of the wave field, $\mathbf{P}_{incident}$ is the up-wave power resource (CgE) computed for the \mathbf{H}_s and \mathbf{T}_p from linear wave theory or within the model and l is the grid length (30m).

The Garden Island field study (Contardo et al., 2017) highlighted the challenges with using transmission coefficients from the industry standard power matrix for the purposes of simulating the WEC performance. In their study they were able to construct a power matrix based on the observations. However, here the industry specified guidelines are used with the rationale that the experiments incorporating the four chosen industry power matrices are designed to provide broad indicative estimates of the impacts.

The power matrices for the first three devices were sourced from Babarit et al. (2011) while the fourth is published in Flocard and Hoeke (2017). Given that the incident wave power (CgE) can be computed from linear wave theory (with \mathbf{H}_s and \mathbf{T}_p), the transmission of the incident wave field through a single device can be calculated with Equation 2. For each device type, the device transmission matrix for a single device in 25m of water is shown in Figure 3.

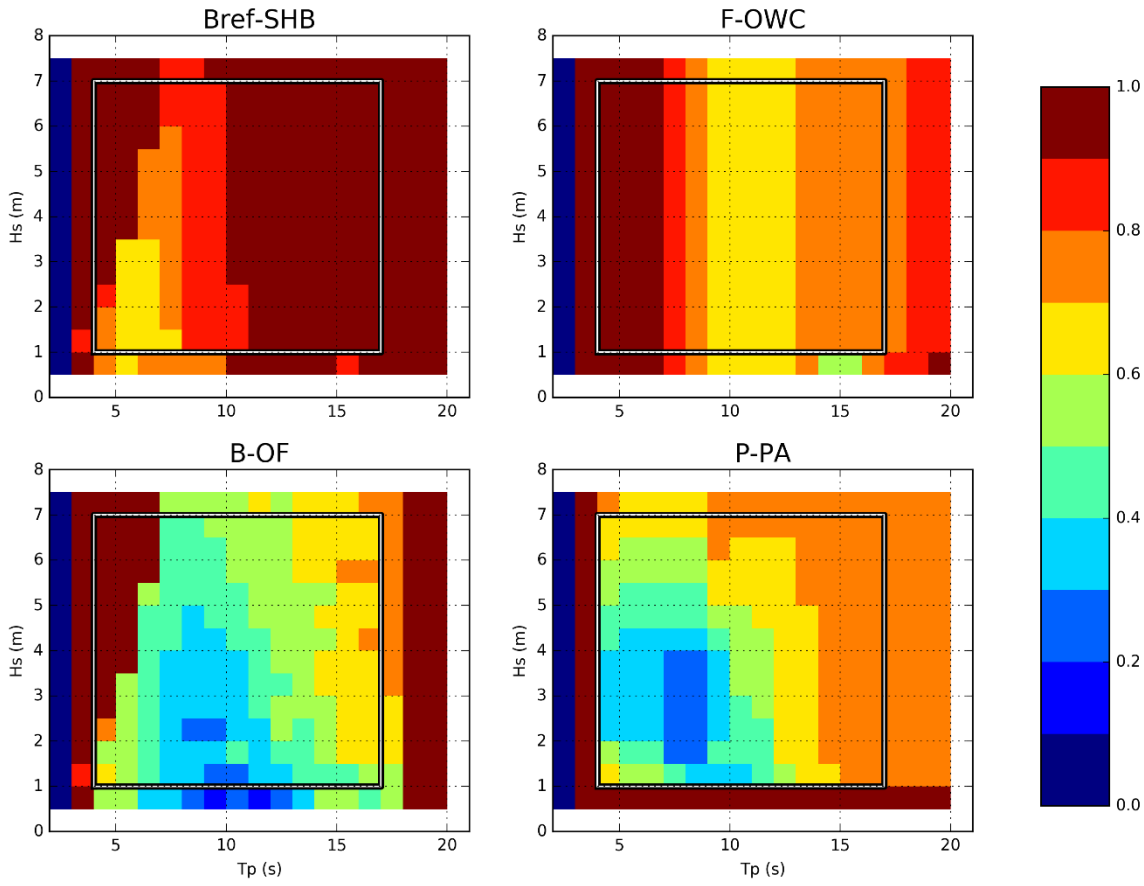


Figure 3 Device transmission factor matrix $K_t^2(H_{m0}, T_p)$, where one indicates full transmission and zero indicates no transmission (full blocking). Absorption is one minus the transmission.

The total electrical power extracted by the array can be formulated as:

$$F_{out}(H_s, T_p) = n \cdot P_{out}(H_s, T_p), \quad (3)$$

where $F_{out}(H_s, T_p)$ is the approximate total electrical energy output by the array with n number of devices. Statistics on the WEC array power output for each considered wave climate / location are presented in Table 6 and were calculated with Equation 3 by sending the four wave climates through the width-normalised power matrix. The nameplate nominal capacity, (i.e. the maximum power output) is rarely returned for the selected climates – thus the array power output (Table 6) is always a fraction of the nominal array size. The total amount of wave power absorbed by the array can be formulated as:

$$F_{absorbed}(H_s, T_p) = n \cdot w \cdot P_{incident}(H_s, T_p) (1 - K_t^2(H_s, T_p)), \quad \text{Equation 4}$$

where $F_{absorbed}(H_s, T_p)$ is the total energy absorbed by the array with n devices. Statistics on the array output for each considered wave climate / location were calculated with Equation 4 by applying the four wave climates to the width-normalised power matrix (Equation 1) to compute the transmission (Equation 2), and then multiplying by the device width (Table 5) and by the number of devices (Table 4). In the

simplified simulations presented, $P_{eff}(H_s, T_p)$ in Equation 1 is unknown and is therefore set to zero, so $F_{absorbed}(H_s, T_p) = F_{out}(H_s, T_p)$.

Table 6 Array power output $F_{out}(H_s, T_p)$ percentile statistics in kW. Note the method for computing array power output is independent of the array configuration or bathymetric slope. Also note that with $P_{eff}(H_s, T_p) = 0$, the values below also correspond to the approximate amount absorbed by the array $F_{absorbed}(H_s, T_p)$.

	50 th				75 th				95 th			
	Albany	Perth	Pt Fairy	Sydney	Albany	Perth	Pt Fairy	Sydney	Albany	Perth	Pt Fairy	Sydney
Bref-SHB												
20 MW	1478	706	1345	794	2154	1232	2496	2040	4220	3204	4829	3677
3 MW	246	118	224	132	359	205	416	340	703	534	805	613
F-OWC												
20 MW	2378	1120	2753	390	3985	2039	4458	1281	7453	4536	9097	2879
3 MW	340	160	393	56	569	291	637	183	1065	648	1300	411
B-OF												
20 MW	3505	1822	3738	894	5052	2816	5985	2226	10382	6498	11318	4270
3 MW	584	304	623	149	842	469	997	371	1730	1083	1886	712
P-PA												
20 MW	4020	1866	4544	1260	6813	3423	7367	3212	11048	8450	12204	6148
3 MW	640	297	723	200	1084	545	1172	511	1758	1344	1942	978

How well a wave energy device is suited to a particular local climate is represented by its efficiency (Table 7). We represent the efficiency by the ratio of power output of a single device for a wave climate to the nameplate capacity at any point in time (Table 3). Note, mean efficiency is equivalent to the device capacity factor. For the 50th percentile climate, the devices are running at less than 25% efficiency with a minimum of 2% efficiency (F-OWC at Sydney) and for the 95th percentile climate they are running at greater than 18% and up to 65% efficiency (P-PA at Port Fairy). Tables 6 and 7 show that B-OF and P-PA are likely to generate the most power output, and extract power closer to their peak efficiency at Port Fairy and Albany.

Statistics on the attenuation of waves through a single device (defined as one minus the transmission factor in Equation 2) is calculated for each location (Table 8). Attenuation down-wave of the array should have a proportional impact to the power extracted by the array. However, due to the dynamic wave field propagating through the array, we are not able to simply approximate the net transmission across the multiple rows (Table 4) of the array. Table 8 show the attenuation for individual devices based on Equation 2. Each Bref-SHB device attenuates between 1% (50th percentile for all locations) to 7% (95th percentile at Sydney) of the width-normalised up-wave resource at the device. Each B-OF device attenuates between 39% (50th percentile at Albany) to 67% (95th percentile at Sydney) of the width-normalised up-wave

resource. The P-PA device has the largest efficiency factor of the four devices tested (Table 7) and leads to the highest array wave power output (Table 6). An individual P-PA device attenuates relatively little energy compared to individual B-OF and F-OWC devices. Although the attenuation of an individual P-PA device is small, the collective absorption of the P-PA array, which is best suited for all the four climates, is as large as the B-OF and F-OWC devices (seen in the change in wave height values down-wave, Figure 8).

Table 7 Array efficiency factor statistics (i.e. the power output for the given climate statistic as a percentage of maximum power output). Note the method for computing WEC array power output is independent of the array configuration, bathymetric slope or array size.

	50th				75th				95th			
	Albany	Perth	Pt Fairy	Sydney	Albany	Perth	Pt Fairy	Sydney	Albany	Perth	Pt Fairy	Sydney
Bref-SHB	13%	6%	9%	9%	19%	11%	17%	22%	38%	28%	34%	40%
F-OWC	13%	6%	13%	2%	22%	11%	21%	8%	40%	25%	43%	18%
B-OF	18%	9%	19%	5%	25%	14%	30%	12%	52%	33%	57%	23%
P-PA	22%	10%	24%	7%	37%	19%	39%	17%	61%	46%	65%	33%

Table 8 Individual device power attenuation factor $(1 - K_t^2(H_s, T_p))$ statistics as a percentage of the available (up-wave) resource. Note the method for computing array power output is independent of the array configuration, bathymetric slope or array size and doesn't represent the net transmission from up-wave to down-wave of the array.

	50th				75th				95th			
	Albany	Perth	Pt Fairy	Sydney	Albany	Perth	Pt Fairy	Sydney	Albany	Perth	Pt Fairy	Sydney
Bref-SHB	1%	1%	1%	3%	1%	1%	1%	5%	2%	2%	2%	7%
F-OWC	21%	20%	20%	25%	24%	24%	24%	29%	31%	29%	31%	31%
B-OF	39%	41%	38%	56%	43%	47%	43%	60%	53%	54%	53%	67%
P-PA	6%	5%	5%	10%	7%	7%	7%	11%	10%	10%	9%	14%

3.5 Numerical Simulation Model

The phase-averaged spectral wave model SNL-SWAN (Ruehl et al., 2015) was selected to perform the simulations. While spectral wave models have known shortcomings, particularly for simulating diffraction and WEC-WEC interaction, their computational efficiency and accuracy at larger space- and time-scales make them arguably the best choice to understand mid- to far-field wave attenuation effects of WECs amongst currently available numerical models (Folley et al., 2012). The SNL-SWAN model is capable of simulating wave frequency (wave period) and wave height dependent transmission (absorption) of wave energy based on user-input power matrices through several different implementations.

The grid resolution was chosen so that the grid cell would be exactly collocated with the devices, and the device length would be smaller than the grid length. At least one grid cell between WECs is required to simulate waves not directly incident on the WECs. Therefore for simplicity in the comparison and to accommodate all devices, the WEC spacing was set to 60m, the row spacing was also 60m, and the grid resolution was set to 30m × 30m for all simulations.

The extent of the model domain is shown in Figure 2. The shore-perpendicular extent was selected to be 6 km to ensure that (1) the offshore boundary was in at least 40m of water for both profiles and (2) the offshore boundary was not too far from the shore for reasons of computational efficiency. The shore-parallel extent was chosen to be 12 km so that waves coming in at large angles would uniformly impact the WEC array. With the grid resolution of 30 m, the resulting grid provided a computationally feasible 200x400 grid points for the thousands of sensitivity simulations.

The model was set up to run simulations for both model domain types (steep and gentle profiles, see last section) with no WECs (baseline) and for each permutation of WEC device and WEC array configuration (total: 34 = 2 domains x (1 baseline+4 WEC types x 4 WEC array configurations)). These simulations were performed for all 500 sea states at each of the four locations (Perth, Albany, Port Fairy and Sydney, see section 5.3), resulting in a total of 68,000 simulations (17,000 at each location).

WEC obstacles are parameterised in SNL-SWAN using a refined definition of obstacle lines crossing grid vertices (SNL-SWAN <http://snl-waterpower.github.io/SNL-SWAN/>). For an obstacle equal to or smaller than the grid resolution, one (or two) line(s) is (are) created to cross two orthogonal grid lines. This means that obstacles will span multiple grid lines and have a 2D shape. The power absorbed as determined by the power matrix is then scaled by obstacle length relative to the grid resolution (always less than or equal to 1). This means their length and transmission effects can be properly captured. The guidelines will focus on bulk wave statistics, so the modelling employs the wave transmission method of obstacle case 1 (equation 2 defined above), which is shown to give similar bulk wave results to obstacle case 3 (Contardo et al., 2017). The definition of each obstacle case is contained in the SNL-SWAN manual.

The use of baseline simulations allows comparison of the different WEC array permutations with conditions where no WECs are present. To analyse how conditions differed (between the presence of WEC arrays and

without) for each of the 500 sea states, the following wave variables were saved as model output from each simulation (The SWAN Team, 2017):

4. Significant wave height (H_s) climate - an easily understandable indicator of change and also related to other wave field parameters, such as wave orbital velocity.
5. Wave power (CgE) - indicates the change in the energy resource.
6. Maximum near-bottom orbital velocity (U_o) - indicates changes to seabed mobility transport or environmental stressors
7. Dissipation due to depth-induced breaking (D_{surf}) - energy dissipation due to surf breaking (in W/m^2) indicates how waves will change near the shoreline.

The output variables were subjected to further statistical processing and analysis to aid interpretation of the results and facilitate comparison of the differences between baseline conditions and the various WEC array simulations. These are described in the next section.

3.6 Analysis Methods and Defining Impact Zones

The simulations are analysed in two ways: (1) through maps of the domain results, allowing a largely qualitative interpretation of the differences between the baseline conditions and the different WEC array permutations; and (2) through defined impact zones. The latter aims to quantify the impact metric/geometry (area or distance) for a change in wave field parameters to assist the design of future array installation studies (see also Appendix F).

Both analysis types focus on the local 50th, 75th and 90th percentiles (quantiles) drawn from the population of (wave climate) output variables (H_s , CgE , D_{surf} and U_o) within each of the four location's simulation domains (Equation F.2). In particular, the 75th percentile is used as a descriptive statistic, as this better facilitates comparison of output variables between the baseline and WEC array cases, since it avoids overly low (local) values of some statistics (e.g. local mean or 50th percentile/median) that may be produced in some areas during certain conditions within the simulation domain (Flocard and Hoeke, 2017). The changes in the percentiles between variables (with and without WEC arrays) can be used directly to assess the impact of the WEC array on the wave field, or to indicate indirectly the possible effects on local transport or marine habitat stressors or the possible impact of the altered wave field on the coastline.

An Impact zone is defined as a change in a wave field parameter in terms of a distance or area down-wave of the WEC installation. In the analysis below, the change in a wave variable as a result of the presence of

the WEC array is presented as a percentage change relative to the up-wave condition. An alternative approach, which is not done here, is to present the change relative to the baseline simulations (Flocard and Hoeke 2017) or to use both the baseline and up-wave normalisation (Contardo et. al. 2017). For most applications, these normalisation methods will not lead to major differences owing to the relatively uniform wave field observed across the idealised domains (see Figure 4 in the next section). Where changes relative to baseline conditions are important (e.g., D_{surf}), we also ensure the baseline conditions are presented to aid interpretation. Given the earlier noted shortcomings of spectral models in this region, the focus of this study is not on the region encompassing the wave array (i.e. the near field) but rather the mid field, which extends from outside the array towards the shore and the far field, which is the region close to the shore (the depth-induced breaking zone).

The impact zone analysis (Appendix F) focuses on changes measured in terms of:

1. Area of impact. (Equation F.3)
2. Distance of impact in the cross-shore (shore-perpendicular) direction where modelled changes are measured from the array towards the shoreline in the mid field (Equation F.4)
3. Distance of impact in the longshore direction (shore parallel) in the far field (Equation F.5) where far field refers to the region within 1 km of the coastline for the gentle profile, and within 500 m of the coastline for the steep profile, in both cases corresponding approximately to the 10m depth contour (Appendix D).

In order to provide first estimates of the potential extent of impact of WEC array deployments on the surrounding wave field, we present a set of semi-empirical exponential equations based on the model data that describe the exponential decay of a variable away from the deployed array, to summarise the results of our numerical model simulations. The development of these equations is described in Appendix F, with coefficients for alternative array configurations presented via a look-up table available in Appendix G.

4 Wave array impact zone analysis

In this section the simulated effects of the wave arrays across the four wave climates (i.e locations) are presented. The first two subsections present maps and transects of statistical summaries of the simulations and provides notes on design consideration for the impact of future WEC array installations. The third section quantifies the impact zones and derives a predictive equation to estimate them.

4.1 Wave climate and nearshore profile

To illustrate baseline conditions, maps of 75th percentile significant wave height (H_s) climate without WEC arrays are shown in Figure 4. As illustrated in Figure 1, the largest values of H_s occur with the Port Fairy wave climate. These maps also indicate that at all locations the largest spatial changes in the H_s wave field (due to depth-induced wave breaking) occur within 1 km of the coastline for the gentle profile (top row), and within 500 m of the coastline for the steep profile, in both cases corresponding approximately to the 10m depth contour (1). It is worth noting there is no active wave-generation by wind within the model domain.

Figure 5 shows the difference in the 75th percentile H_s climate (Equation F.1 and F.2) between the baseline and the simulations with an array of 44 P-PA devices in the 20 MW square multi-row array configuration for the Perth climate with the two bathymetric profiles. This illustrates that in the case of the steeper bathymetric profile (plot on right), the WEC array is closer to the coast, and so the magnitude of the attenuation in wave height is also greater closer to the coast relative to the gentle profile (shown on left). This also limits the spatial extent of the impact relative to the gentle profile, i.e. while the magnitude of the impact to the wave field is greater closer to the shoreline in the steep profile, the area impacted by the WEC array is greater in the gentle profile.

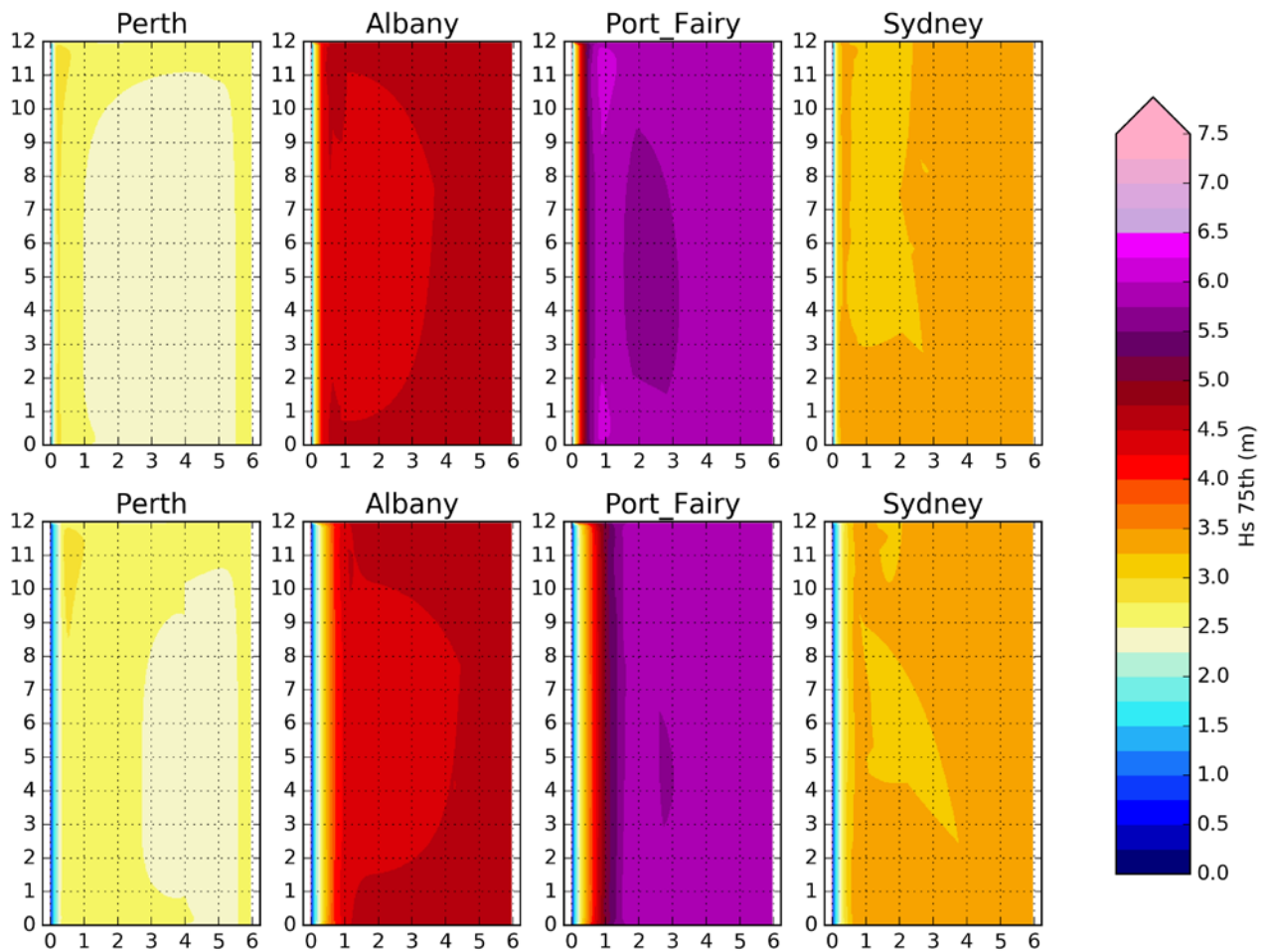


Figure 4: 75th percentile climate maps of H_s (m) for the four locations (columns) and for the steep (top row) and gentle (bottom row) bathymetric profiles. The coast is on the left and the figure extends to 6 km offshore.

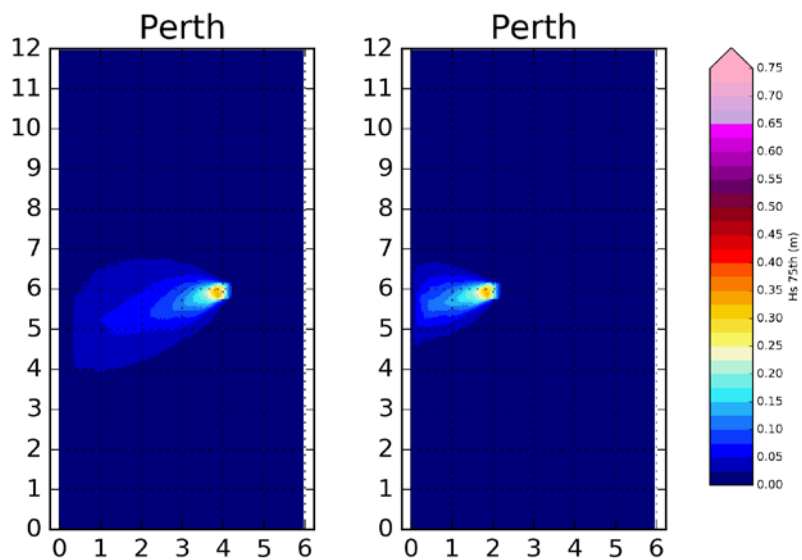


Figure 5: Maps of change in the 75th H_s climate for the gentle bathymetric profile (left) and steep profile (right) for the P-PA 20 MW square row array for the Perth wave climate. The control wave height values are presented in Figure 4.

The difference in the 75th percentile H_s climate between the baseline and WEC array simulations with the P-PA device in the 20 MW square array is shown for each of the four wave climates with the gentle profile in Figure 6. The amount of down-wave attenuation depends on the incident H_s and T_p climate, and how that passes through the $P_{absorbed}$ matrix (Equation 2). Typically larger absolute attenuation will occur in locations with larger H_s climates (Babarit et al., 2012). Transmission matrices adopted for the study have no directional dependence. For some devices (e.g. pitching devices), directionality of waves may be an important factor which is not captured by this study.

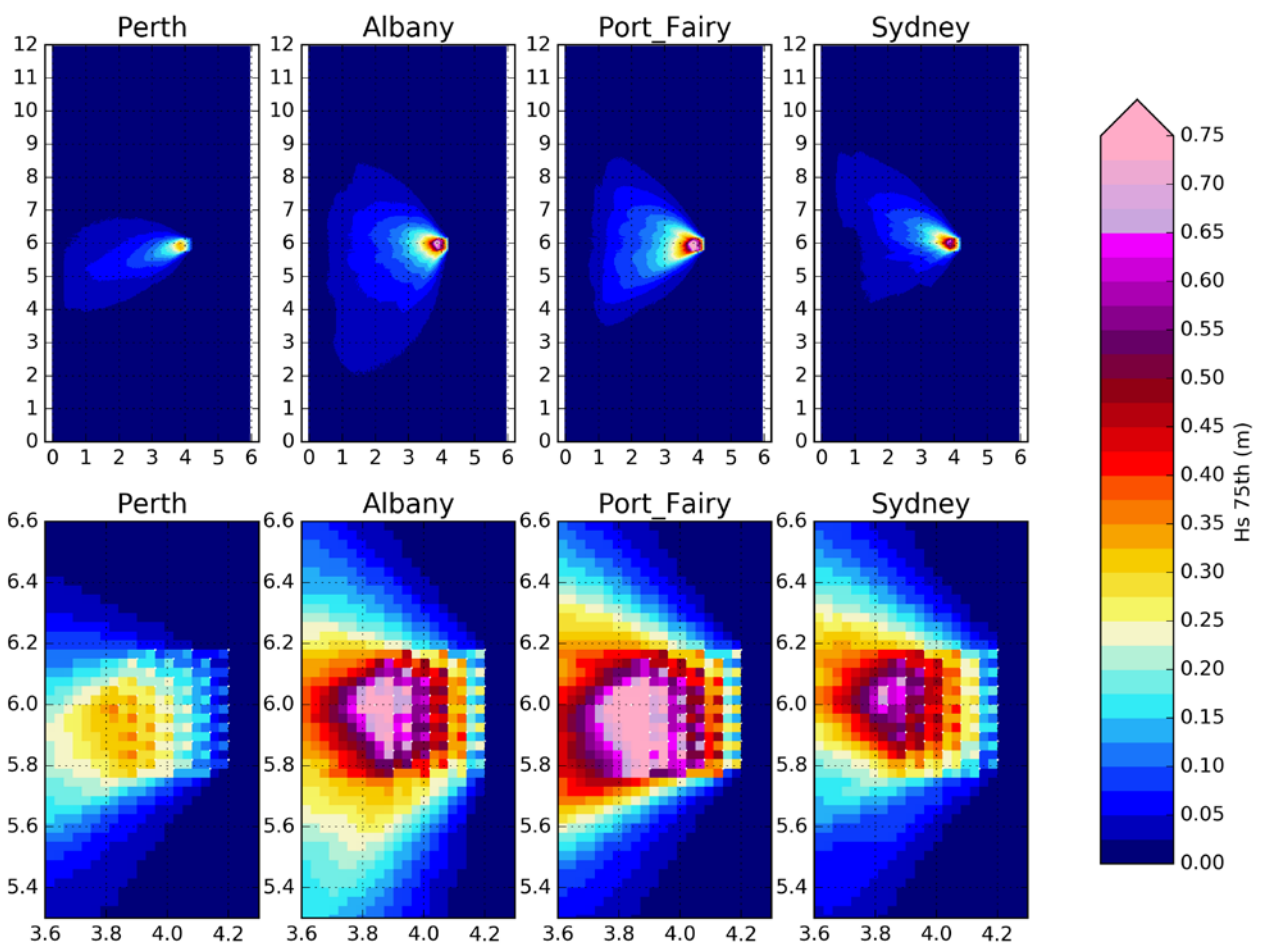


Figure 6 Maps of change in the 75th H_s climate. Same as previous figure but for four different climates, and for the gentle profile only, using the P-PA 20 MW square row array. Top row is the full model domain showing the mid-field attenuation and the bottom row shows an enlargement over the array. Control wave height values are presented in Figure 4.

4.2 WEC array configuration

Figure 7 shows the maps of change in the 75th H_s climate for 20 MW P-PA array in the two-row configuration. In this case, the area of large H_s attenuation (H_s change above 0.5 m) that occurred for the square array (Figure 6), is not apparent. Instead, moderate H_s attenuation (H_s change less than 0.5 m) occurs over a wider extent for the two row configuration. Each device in the two row configuration has more incident (uninterrupted) wave energy than the square array formation so that as the waves approach each row of WECs in the square row configuration there will be less incident wave energy available, potentially resulting in less power output (ignoring possible WEC-WEC interaction).

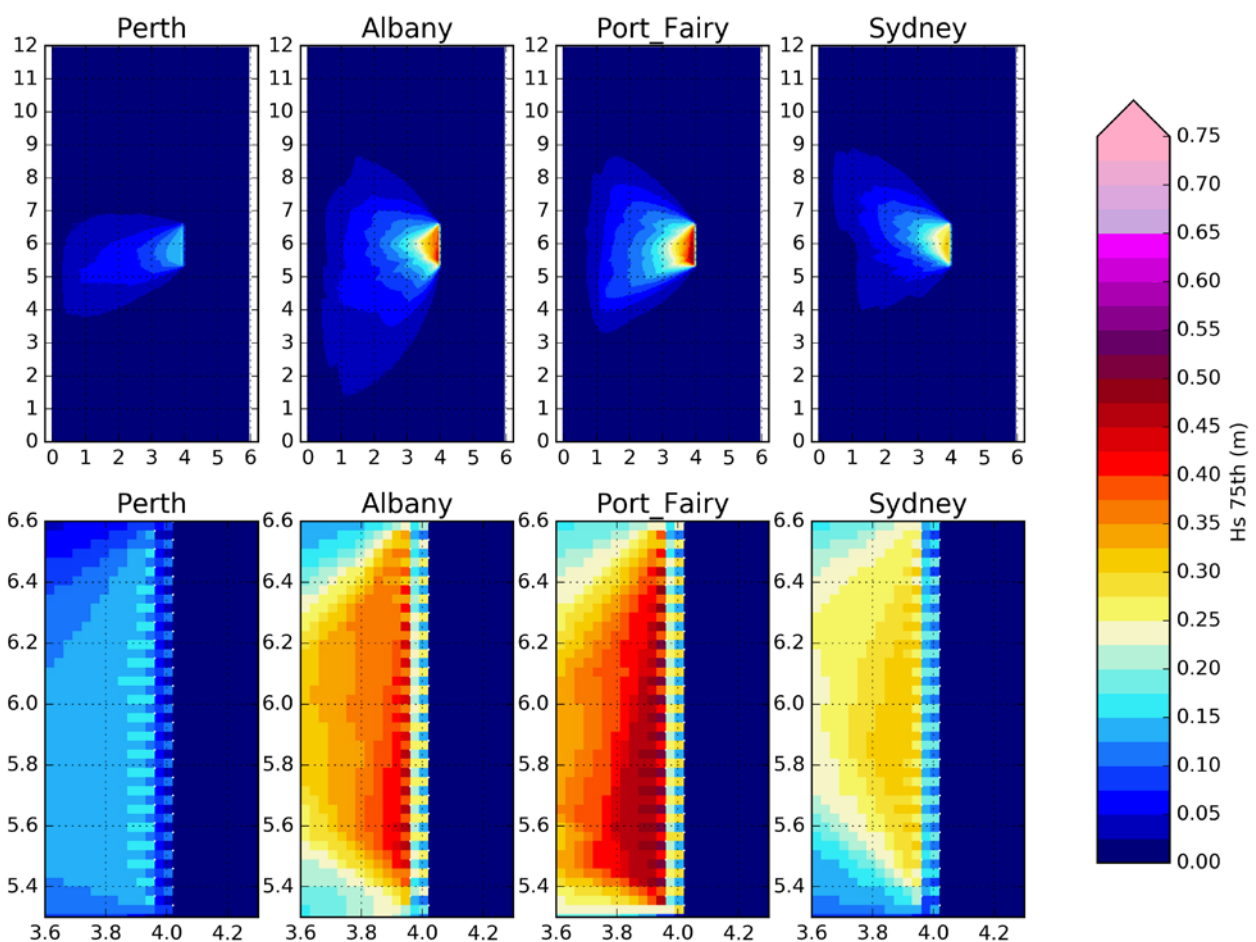


Figure 7 Same as previous figure but devices are in a two row array configuration instead of multi-row square configuration (see Figure 6). Control wave heights are presented in Figure 4.

The transmission factor, or the percentage of energy absorbed as the waves pass through the square array is complex. As the wave progresses through the array and interacts with successive rows of WECs H_s reduces and the sea state enters different cells of the transmission power matrix (Figure 1). This can result

in increased or decreased transmission depending on the wave climate and the power matrix of the particular WEC design. For example, for the P-PA devices, 50-60% of the energy of 6 m 7 s waves would be transmitted (40-50% absorbed), resulting in 3-4 m 7 s waves, of which only 20-30% would then be transmitted (70-80% absorbed) in the next row of devices. The pattern of transmission varies for each device.

The cross-shore transect (Appendix F equation F.4) of the simulated change in the 75th percentile H_s climate is shown for the 20 MW square array for all device types, all climates and both bathymetric profiles in Figure 8. The H_s attenuation associated with the P-PA WEC array (Purple lines) shows incremental steps of increased attenuation as the waves pass through the rows of devices in the near-field, followed by reduced attenuation of the signal at locations further down-wave from the array due to the mixing of waves from oblique angles. The P-PA has the third highest near-field attenuation for all climates except for Sydney (bottom row of plots), where it is second highest because the F-OWC device (red line) blocks less energy for the shorter period waves, which are more prevalent in the Sydney wave climate (Figure). For the 20 MW arrays presented in Figure 8, the order of attenuation of device type (high to low) 1km down-wave of the array, ($x = 3000$ m for the gentle and $x = 1000$ m for the steep profile) follows the same order as the total power output by the array (Table 6). These figures indicate the devices with larger nameplate capacity that extract the required resource using fewer WECs (red and green lines) have a more intense impact (i.e. H_s change greater than 0.5 m) at the array (near-field) than devices with smaller nameplate capacity that are deployed in greater number to achieve the same energy extraction. The latter deployments have a less intense (H_s change less than 0.5 m) impact spread over a wider extent. Down-wave from the WEC array, the larger nameplate capacity devices that extract the required resource using fewer WECs, have a smaller array extent in the longshore direction, hence block less waves for oblique angles than the devices using a greater number of WECs, so the attenuation down-wave of the device drops off more quickly down-wave of arrays with fewer devices.

The pattern or signal attenuation shown for H_s in the previous figures, i.e. large changes at the device and more gradual decay of the signal down-wave of the device, is also reflected in equivalent figures of CgE and Uo shown in the supplementary plots (Appendix H). The down-wave reduction (attenuation) in wave height due to the presence of the array results in some waves remaining unbroken until they are closer to the shoreline, leading to regions of reduced wave-breaking energy compared to the control simulations (Figure 9). This may result in changes in sediment transport and subsequently shoreline position. The steeper profile has a narrower region with more intense reduction in breaking compared to the gentle profile.

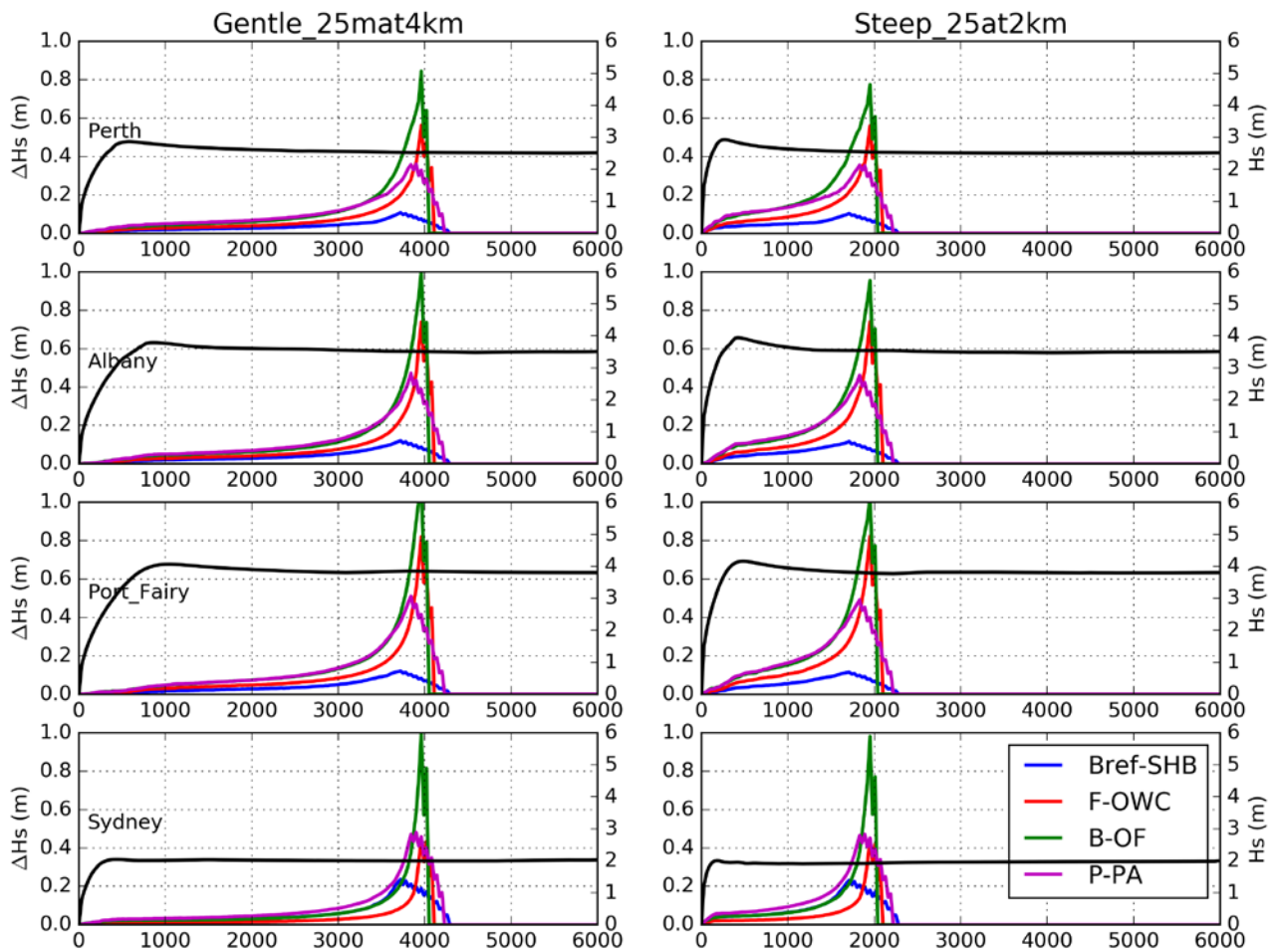


Figure 8 Cross-shore transects of the change in H_s (ΔH_s) for the 75th percentile baseline H_s and the 20 MW square array configuration. Positive values represent attenuation of wave height. Right (left) columns represent the gentle (steep) profile and each row represents a different wave climate. Note that the left vertical axis represents ΔH_s shown by the coloured lines and the right axis represents the baseline H_s shown by the black solid line.

In addition to the cross-shore changes, we also consider the lateral, or long-shore changes observed in response to the deployment of the WEC array (Equation F.5). Here we present changes observed within the 10 m depth contour. The 10 m depth contour occurs approximately 500 m (1000 m) offshore, or 1500 m (3000 m) down-wave of the WEC array, for the steep (gentle) profile domains. The simulated changes in the 75th percentile D_{surf} climate in the nearshore, longshore transect for the 20 MW square array for all device types, all climates and both bathymetric profiles are shown in Figure 10. The plots show that the maximum attenuation of D_{surf} as a response to the presence of the WECs is directly down-wave of the arrays, with the attenuation decreased with distance longshore (in both directions). We see greater impact in D_{surf} in the steep profile simulations where the WEC array is closer to the shore and breaking is stronger. In the gentle slope simulations, the wave field has largely recovered to its natural field at the point of breaking 3000 m down-wave of the array (through contribution of oblique waves behind the array), and so the change to the

breaking wave force is minimal (although greater longshore effects in the gentle slope simulations can be observed). The long-shore extent of impact is dependent on the wave climate. For example, Sydney's highly variable directional wave climate results in a much wider longshore area impacted, although values are smaller owing to the less energetic wave climate of this site.

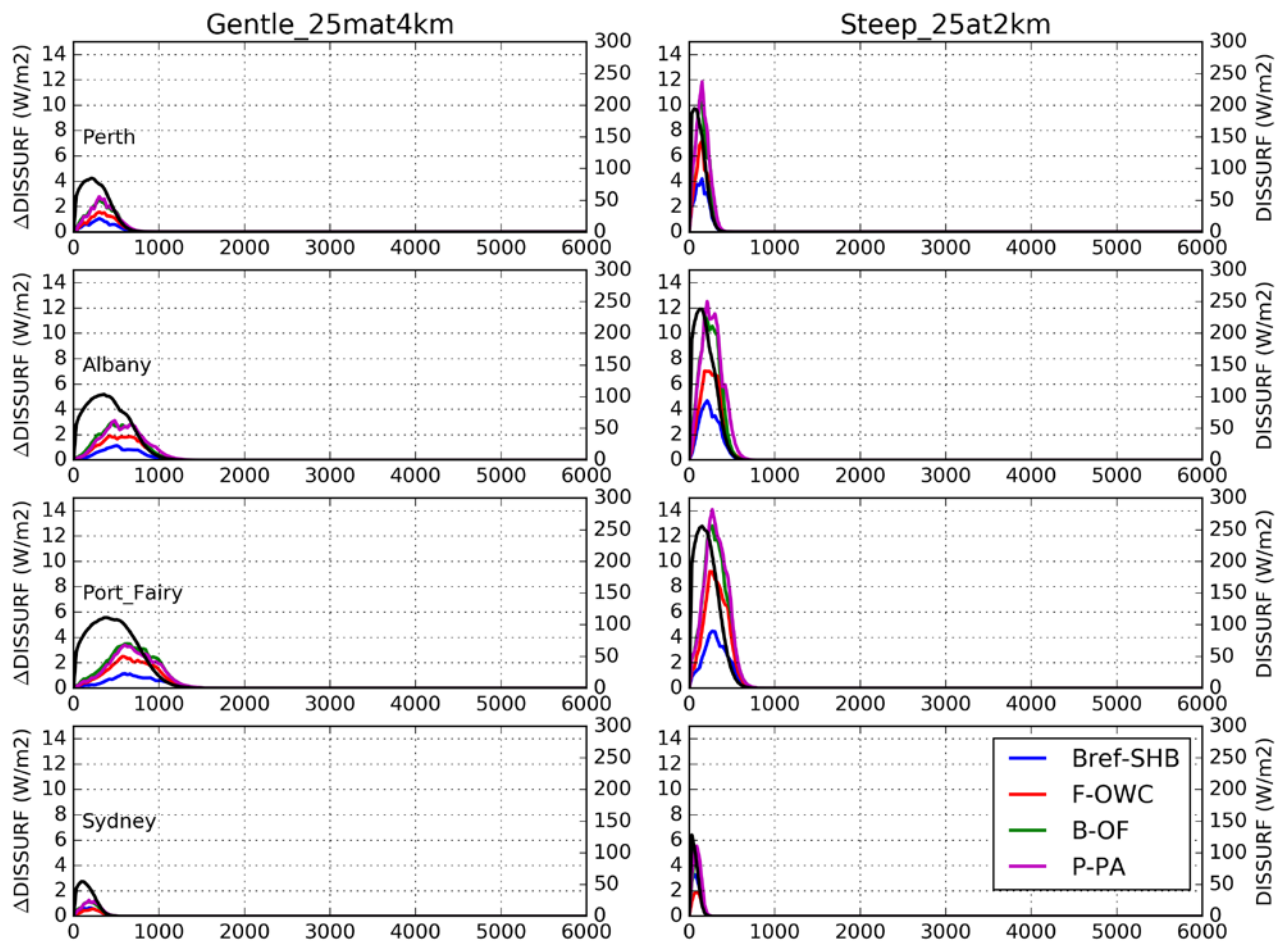


Figure 9 Cross-shore transects of the change in D_{surf} (ΔD_{surf}) for the 75th percentile baseline H_s and the 20 MW square array configuration. Positive values represent attenuation of D_{surf} . Right (left) columns represent the gentle (steep) profile and each row represents a different wave climate. Note that the left vertical axis represents ΔD_{surf} shown by the coloured lines and the right axis represents the baseline D_{surf} shown by the black solid line.

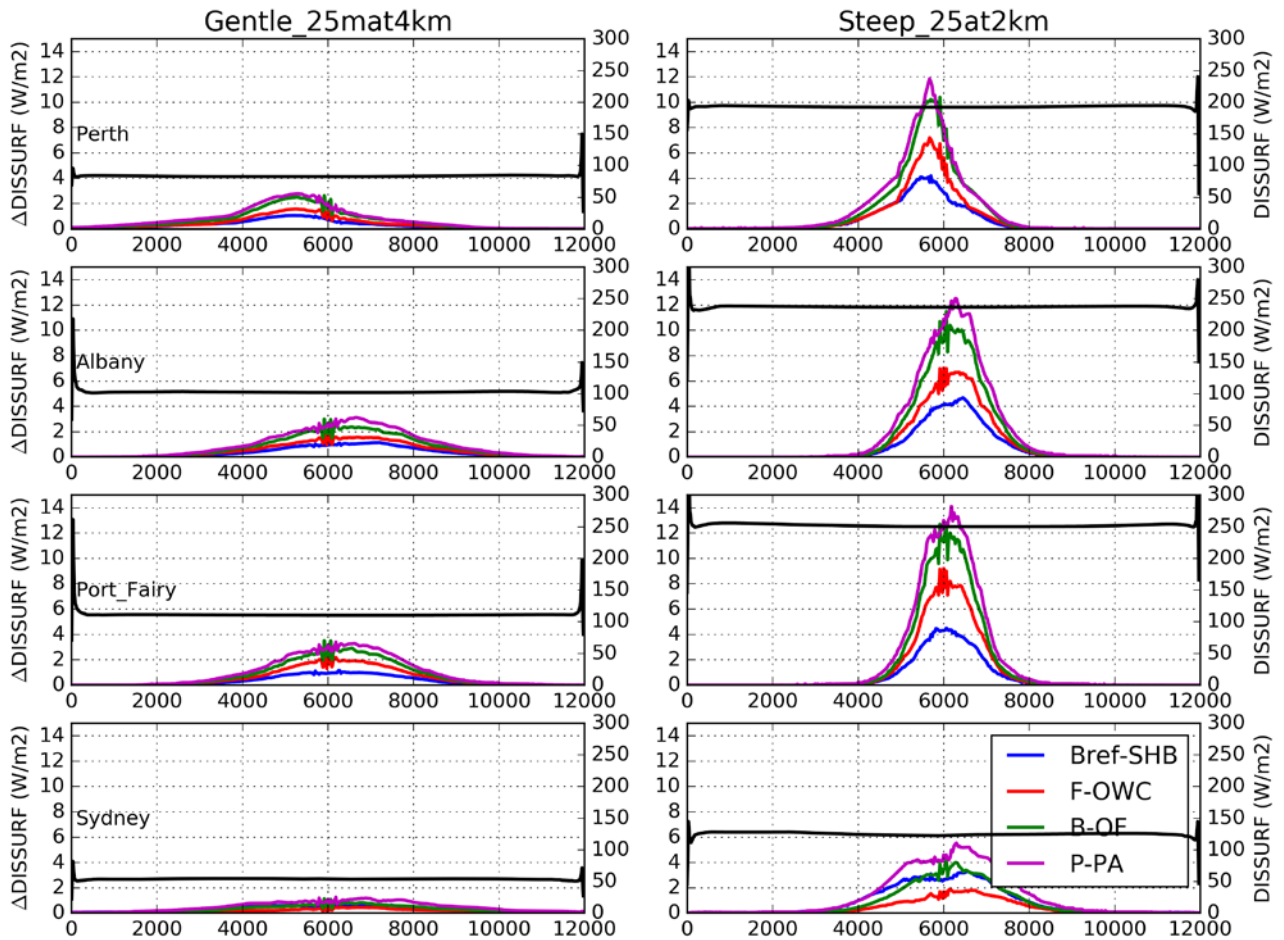


Figure 10 Shore-parallel transects of the change in D_{surf} (ΔD_{surf}) for the 75th percentile baseline H_s . For the 20 MW square array configuration. D_{surf} shows region of decreased wave breaking. Note black line corresponds to the maximum value of D_{surf} as shown in the cross-shore profile in Figure 9.

4.3 Semi-empirical equations for quantifying down-wave impact.

In this section, we summarise the results from all permutations of the array configurations and wave climates (locations) in terms of how the local down-wave variables (H_s , CgE , Uo and D_{surf}) are changed relative to baseline simulations. These impact zone metrics are more rigorously defined in Appendix F.

A comparison of impact distance in the cross-shore direction (ICS, Equation F.4) for the different WEC array configurations and wave climate locations is presented in Table 9 for H_s . This table illustrates the distance down-wave from a given WEC array that the 75th percentile up-wave H_s climate is reduced by 5% or more. The order of the device type attenuation (high to low) of the 20 MW arrays in the square row configuration follows the order of the total power output (absorbed) by the WEC array (Table 6). Different array configurations, device types or wave climates contribute to the different ICS distances. For example, there

is a nearly 100% difference in the distance that wave height is attenuated by 5% down-wave of a 3 MW single F-OWC (60 m) and the single B-OF (120 m) device deployed in Sydney's wave climate. So when comparing these two single devices we can attribute the difference to the attenuation factor (Table 8) which is 29% for F-OWC and 60% for B-OF for Sydney's 75th percentile wave climate. In the case of the larger array with multiple devices, the relationship to the individual device attenuation factor (Table 8) is not uniform due to the multi-row spatial positioning of the devices and the influence of waves approaching from oblique angles around the array of WECs. In this case, a reduction of 5% is selected as an example of acceptable impact (e.g. similar to Chang et al, 2014), and is used for demonstration only. Depending on the application, alternative reductions (e.g., 1 or 10%) might be more appropriate for impact assessment. The impact response to different choices of reduction percentages is non-linear because of the different array configurations and the devices ability to attenuate the up-wave field (Table 8). For example, it does not necessarily follow that if the distance associated with a 5% reduction for one array type is larger compared to another array type that this relationship holds for different percentage reductions. This is illustrated in Figure 8 where for the Sydney wave climate (bottom row), the choice of a 20% reduction (0.4 m) for a noticeable impact would suggest the B-OF device (green line) would lead to a larger cross-shore (ICS) impact distance (within the near-field) than the P-PA model (magenta line). However, if a 10% reduction (0.2 m) were chosen, the ICS distance would be greater for the array of P-PA devices. Our confidence in the near-field effects is limited, and in the mid-field, a similar response is seen between these two devices.

For large nameplate capacity devices (Table 3) that require fewer devices to reach the configured array size (e.g. F-OWC and B-OF require 6 and 7 devices for a 20 MW array), the difference in array configuration (two row or square) has little to no influence on the ICS distance. For smaller nameplate capacity devices, which require large arrays to reach the configured array size (e.g., Bref-SHB and P-PA), there can be a significant difference in ICS distance dependent on whether the array is configured in a deep square (Figure 8) or wide two-row (Appendix H Figure I-3) array. The ICS distance in the two-row configuration is almost always lower, and in some cases there is no impact evident at the 5% level, whereas the square array has ICS distances of several hundred metres as is seen for a 20 MW array of P-PA devices at Albany (Figures 8 and Table 9).

Table 9 Impacted cross-shore (ICS) distance (m) for a 5% reduction relative to the incident significant wave height (H_s) for the 75th percentile climate. Columns represent the wave climate location and bathymetry and the rows indicate the type of WEC, array size and configuration. These distances include the spatial size of the array, e.g. a two row array with more than one device has a cross-shore distance of 60m plus the device width.

Row Labels	Albany		Perth		Port_Fairy		Sydney	
	Gentle	Steep	Gentle	Steep	Gentle	Steep	Gentle	Steep
Bref-SHB								
20 MW_large								
square_row	0	0	0	0	0	0	720	750
two_row	0	0	0	0	0	0	0	0
3 MW_small								
square_row	0	0	0	0	0	0	0	0
two_row	0	0	0	0	0	0	0	0
F-OWC								
20 MW_large								
square_row	480	510	600	660	480	540	330	330
two_row	480	510	600	690	450	510	300	330
3 MW_small								
square_row	90	90	90	90	90	90	60	60
two_row	90	90	90	90	90	90	60	60
B-OF								
20 MW_large								
square_row	660	750	900	1,140	660	780	600	630
two_row	630	720	960	1,230	690	810	570	570
3 MW_small								
square_row	120	150	150	150	150	150	120	120
two_row	120	150	150	150	150	150	120	120
P-PA								
20 MW_large								
square_row	780	840	1,050	1,230	750	870	1,020	1,080
two_row	60	0	480	510	0	0	1,050	1,110
3 MW_small								
square_row	30	30	60	90	30	30	210	210
two_row	0	0	30	30	0	0	180	180

The cross-shore distance impacted is dependent on what change is of interest. i.e., a large decrease in wave height will be felt over only a short distance away from the array, whereas a small decrease in wave height may be felt over a longer distance. To demonstrate this relationship, we plot the modelled ICS distance relative to the down-wave H_s change for the 50th 75th and 95th percentile H_s of a two-row 20 MW array on a gentle profile (Figure 11). The curves, coloured by the power output by all devices in the array (total array

power output Table 6), represent simulations for all considered wave climates (four locations, and three H_s percentile levels and four device types). The results indicate a general pattern whereby larger WEC power outputs lead to given changes in wave height over greater cross-shore distances. This pattern is not apparent in all cases shown in Figure 11 due to complexities in the array configuration. These include the situation where the grouping of runs are limited by the non-linear (strongly dynamic) relationship between impact and bathymetric slope, array configuration (number of rows) and number of devices. The impacts for each grouping are compared to the up-wave parameter (H_s or CgE) where the effects of wave period on the power output are not directly included in the comparison due to the non-linearity of power out with increasing wave period in the device power matrices.

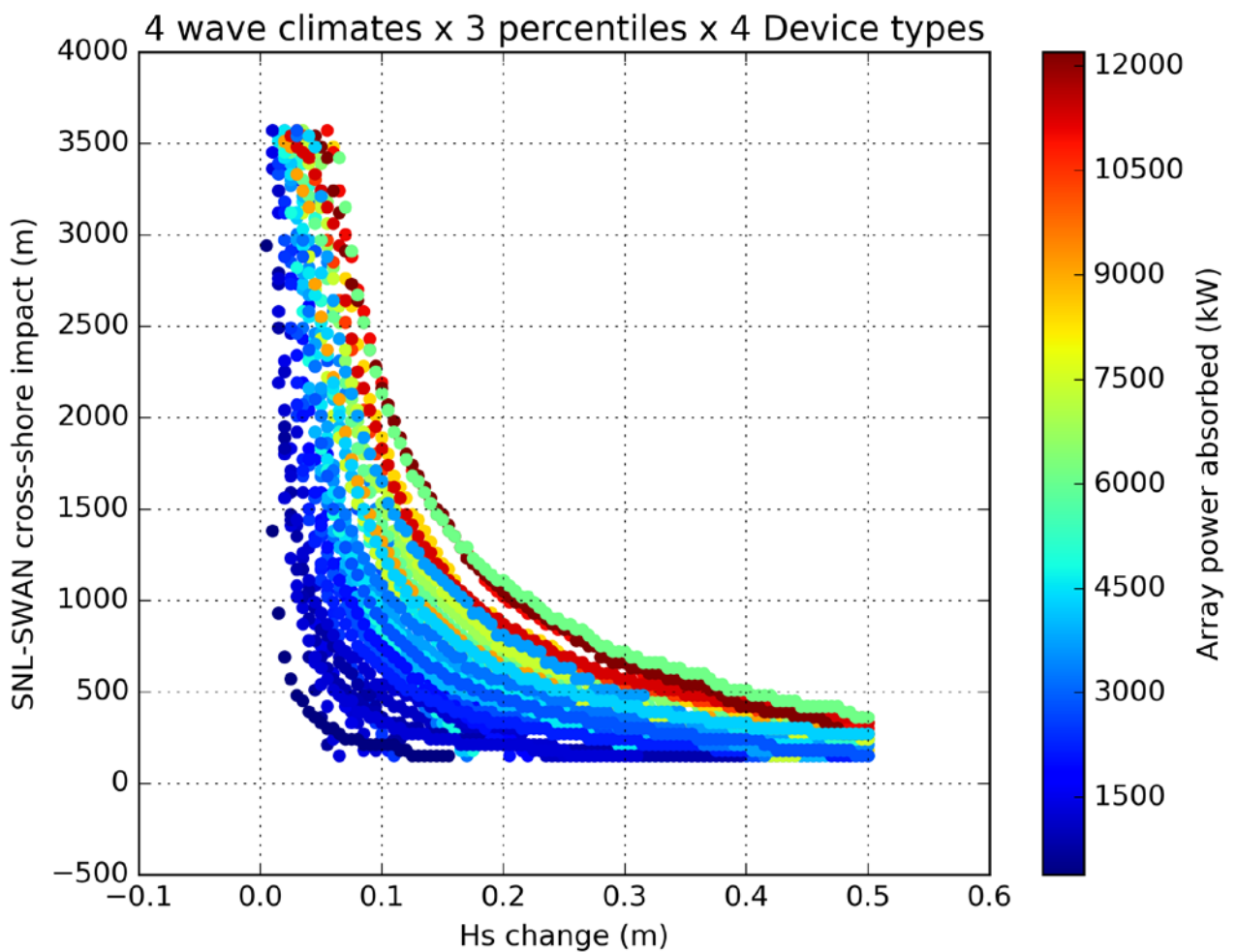


Figure 11 SNL-SWAN cross-shore impact distance plotted against change in H_s . Colours represent the total multi-device power absorbed by the array. Values are for all wave climates, the 50th 75th and 95th climate and for all device types in the 20 MW two row array for the gentle profile.

Alternatively viewed, Figure 12 provides a more accessible 'lookup' table, where down-wave change in wave height (colour scale) is presented as a function of the array power output (x-axis; e.g., Table 6) and cross-shore distance (y-axis).

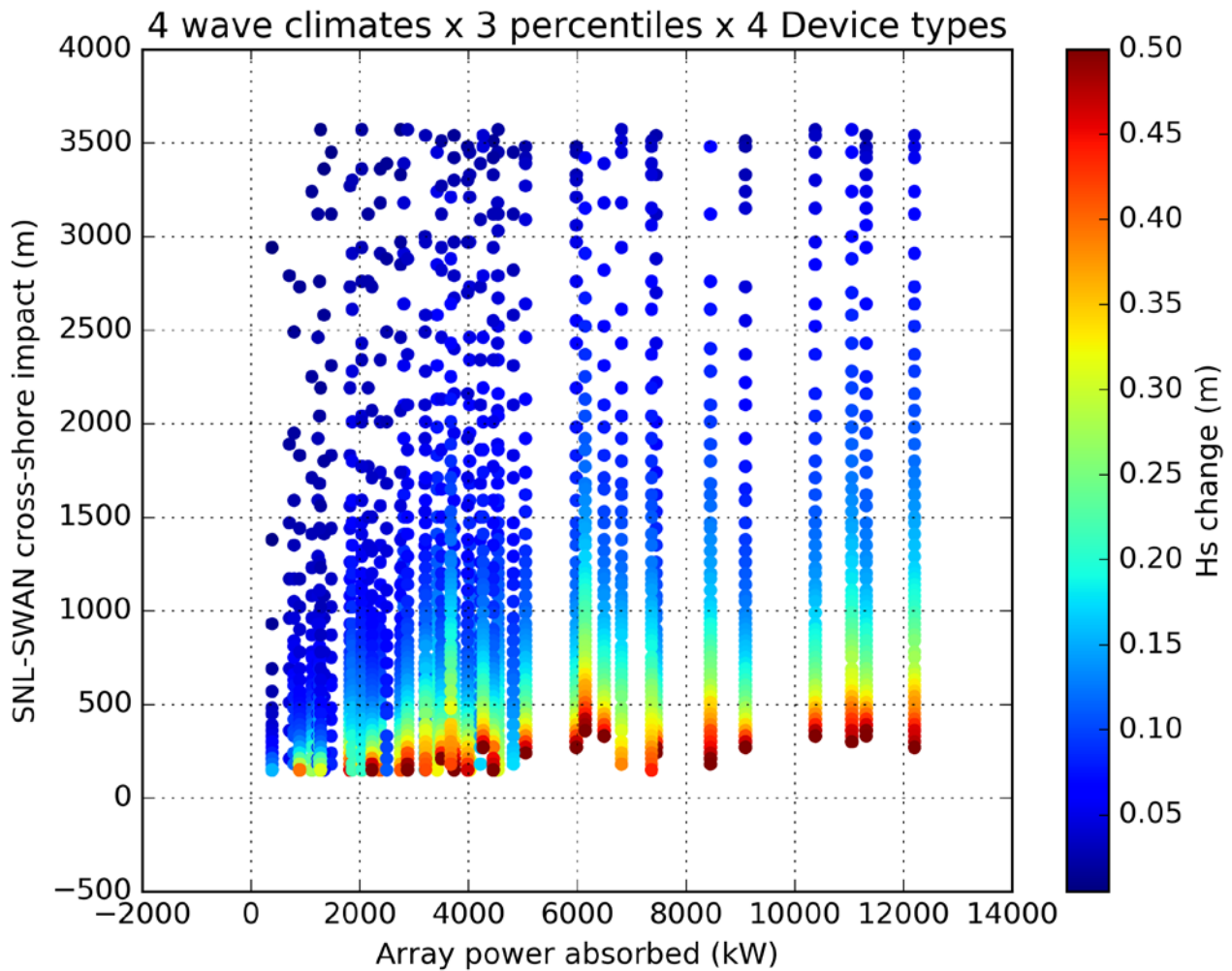


Figure 12 SNL-SWAN cross-shore impact distance plotted against change in array absorption (equation 4). Colours represent the impacted-change in H_s . Values are for all wave climates, the 50th 75th and 95th climate and for all device types in the 20 MW two row array for the gentle profile.

To achieve the objective of providing first-order estimates of the spatial extent of environmental effects of WEC array deployments, the results of the 68000 numerical simulations have been summarised in a simple, usable manner. Here, we provide details for a set of semi-empirical equations derived to describe the potential impact (in terms of area, cross-shore or longshore distance) on a given down-wave wave parameter (H_s , CgE , U_o or D_{surf}), for any combination of input parameters (wave parameter, change in wave parameter and array power output) (Appendix F). The set of equations provide a simple means to estimate

the impact of different combinations of arrays in different environmental settings as a starting point to inform project stakeholders, and identify the spatial extent over which further consideration may be required. Input parameters for the equation include the incident wave height (H_{s0}) and wave period (T_{p0}), to determine the array absorption (Equation 4) and the impacted-change in H_{s0} , ΔH_s (or % H_{s0}). The equations are derived from the set of numerical experiments, to be independent of (i.e. averaged across) device type (power matrix), and wave climate variations (i.e., spread of incident direction). Thus, for any estimated value of impact extent (the output variable of the derived equations), a standard error (rmse) is provided, which captures the uncertainties associated with device specifications and wave climate differences.

The equation (Appendix F Equation F.6) to predict the cross-shore impact distance for H_s is defined as:

$$ICS(\Delta H_s, F_{absorbed}) = a \cdot \exp(b \cdot \Delta H_s F_{absorbed}^{-c}) + d \quad (5)$$

where ΔH_s is the selected impacted-change in wave height (% H_{s0}) and $F_{absorbed}$ (Equation 4) is the expected power absorbed by the array for incident (H_{s0} and T_{p0}) wave conditions. The coefficients a , b , c and d have been empirically-derived from the set of numerical simulations, and are provided in Appendix G. Different sets of coefficients are provided for a range of considerations, including differences in:

- The variables (H_s , CgE , Uo , or D_{surf}) for which the impacts are being considered
- The spatial impact (cross-shore or longshore distance and area of impact)
- The bathymetric profile of the site of interest (steep or gently sloping)
- The array size (small number of devices [less than 16] in the 3 MW or a large number of devices [>16 and < 100] in the 20 MW array)
- Array configuration (2 row or square).

The semi-empirical estimate of impact using Equation 5 for a 20 MW array deployed in a 2-row configuration on a gently sloping profile shown in Figure 12 is presented in figure 13. To illustrate the skill of the semi-empirical model fit relative to the numerical simulations, Figure 14 presents the impact distance cross-shore in H_s , for a 20 MW array deployed in a 2-row configuration, on a gently sloping bathymetric profile. It can be seen that the semi-empirical fit underestimates the results of the numerical simulation, but this difference is largely captured by the quoted error value. Similar plots are presented for all considered scenarios (coefficient sets) in Appendix G.

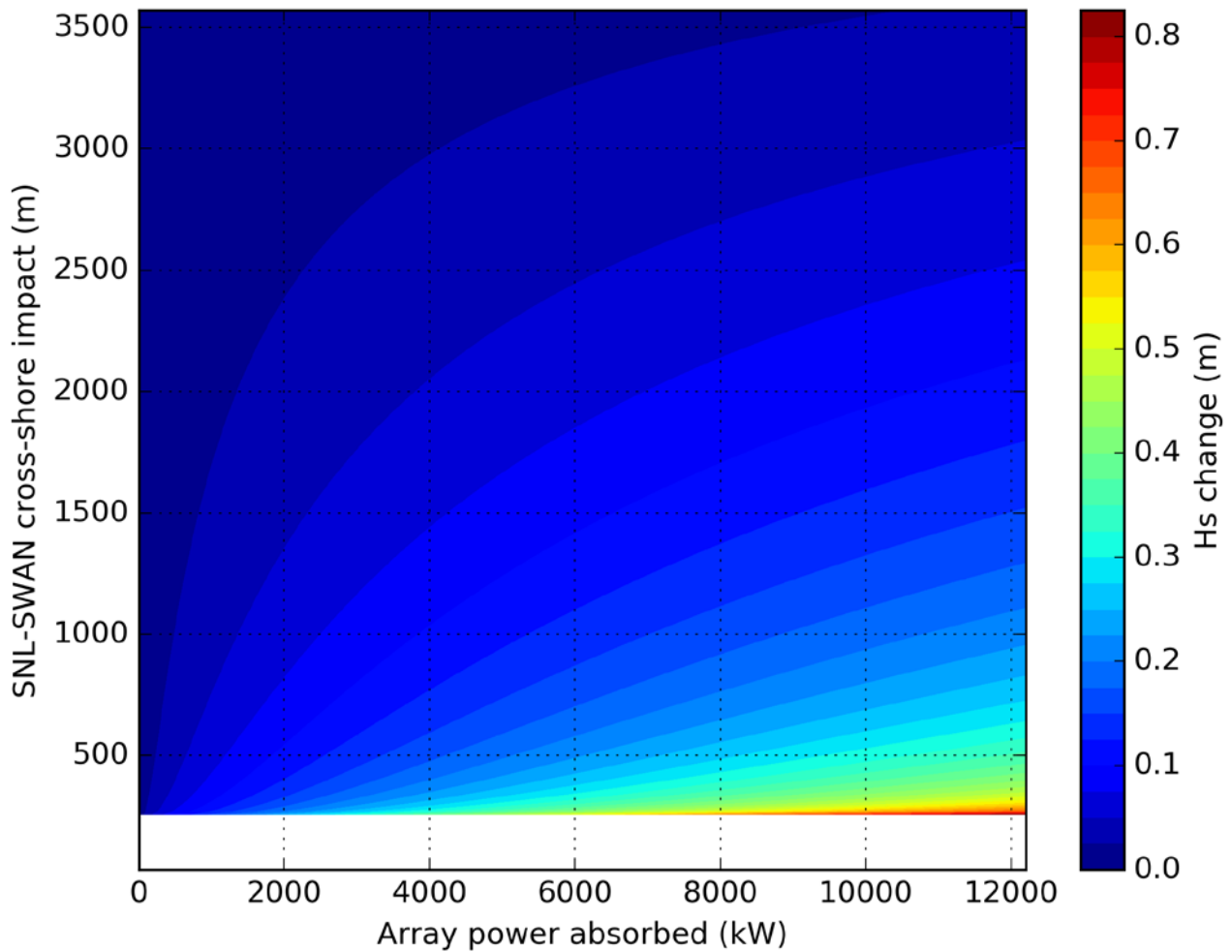


Figure 13 Semi-empirical cross-shore impact distance plotted against change in array absorption (equation 4). Colours represent the impacted-change in H_s . Values are for all wave climates, the 50th 75th and 95th climate and for all device types in the 20 MW two row array for the gentle profile.

Here, the application of the derived semi-empirical equations is demonstrated. We present a scenario where the interest is in the cross-shore distance over which H_s is reduced by 5% or more down-wave of a deployed WEC array. We consider incident H_s of 2 m and 8 s peak period, so that a 5% decrease corresponds to 0.1 m lower wave height and the corresponding incident wave power in 20 m of water is 19.93 kW. An array of 60 WECs is proposed where each WEC is 20 m wide. Each device has been independently measured to transmit 50% of the wave field through the device for these wave conditions. Using Equation 4 the total power absorbed by the array is $60 \cdot 20 \cdot 19.93 \cdot 0.5 = 11958$ kW. The array is similar to the large 20 MW array in a 2 row configuration, deployed on a gently sloping bathymetric profile. Referring to Appendix G, the respective coefficients a , b , c and d are 4030.35, -2430.42, 0.6, 250.56 respectively, and the standard error is 279.64. Inserting $\Delta H_s = 0.1$ m (5% of 2 m) and $F_{absorbed} = 11958$ kW into Equation 5 with relevant coefficients, we obtain the cross-shore distance impacted down-wave of the array:

$$ICS = 4030.35 \cdot \exp(-2430.42 \cdot 0.1 \cdot 11958^{-0.6}) + 250.64$$

which yields an impact distance of 1940.6 m for a 5% change in H_s with a standard error of 203.37 m. This value corresponds to the approximate lookup value in figure 13.

The impact semi-empirical equations can also be rearrange algebraically to find the impact change ΔH_s (or % H_{s0}) for a selected impact-distance ICS:

$$\Delta H_s(ICS, F_{absorbed}) = \frac{F_{absorbed}^c}{b} \log\left(\frac{ICS - d}{a}\right) \quad (6)$$

where for the same design we now consider what the change in H_s will be 500 m down-wave of the array (ICS = 500). This results in an H_s change of 0.32 m, corresponding to 16% of the 2 m up-wave condition.

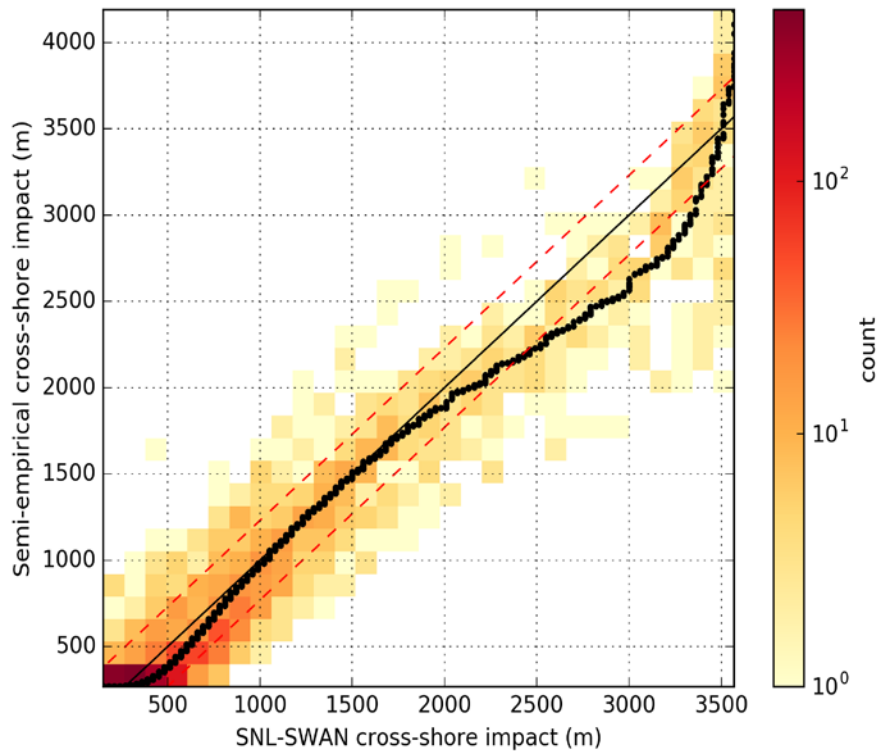


Figure 14 Regression plot of H_s cross-shore impact (ICS) distance estimates for the 20 MW array in the two row configuration for a gentle profile. Colours indicate the density of agreement (count of a 2d histogram). Black dotted-line plots the ordered semi-empirical values against the ordered SNL-SWAN values. Red dashed lines are \pm root mean square error (rmse) to the model fit. Values are for all wave climate locations, the 50th, 75th and 95th climate statistic and for all device types in the 20 MW square row array for the gentle profile.

5 Summary and Next Steps

Environmental impact assessments are a critical part of the wave energy approvals process. They must be undertaken for a development to proceed and are important for building social licence to operate.

However the industry has acknowledged a lack of tools and guidelines to assist with the assessment of potential impacts in the marine environment. This in turn can lead to costly delays in the approval process (Hemer et al., 2017).

The extraction of wave energy by an array of devices has the potential to alter the characteristics of the surrounding wave field with potential flow on effects to the physical and ecological environment. Reduced energy in the wave field may have both negative and positive effects depending on the values ascribed to the coast. For example, reduced wave energy may adversely impact the amenity of a coastal location for recreational activities such as surfing, yet may reduce sediment mobility and hence help reduce erosional effects that threaten coastal infrastructure. Changes in sediment mobility may drive other impacts, both negative or positive, on seabed habitats and local coastal ecology.

The potential impacts of a WEC array will vary according to the specific attributes of the local environment in which it is to be situated. Therefore, a generic tool that can be applied to assess a wide variety of potential impacts was sought to facilitate the assessment of impact zones. For reasons of computational efficiency in carrying out thousands of simulations of WEC array scenarios, the SNL-SWAN model was used as the basis for building the generic tool. Some key limitations of this modelling approach should be noted. Being a phase-averaged wave model, The SWAN-SNL model poorly captures diffraction of waves around the in-water obstacles. Thus, while the frequency dependent transmission of energy through the WEC array can be parameterised, and thus provide estimates of the mid-to-far field effects on the wave field with reasonable accuracy, the near-field effects surrounding the WEC array are not expected to be well captured. Further to the well understood issue of diffraction with phase-averaged models, the application of these models to wave energy problems is also hampered by the lack of parameterisation of radiated waves from an individual WEC, and associated WEC array effects (Chowdhury & Mannaseh, 2017). The effects of these limitations are expected to be more strongly felt in the near-field around the WECs. Validation of the SWAN-SNL model with data collected from down-wave of an in-sea deployed WEC array (Contardo et al., 2017) supports this expectation, and provides justification for the application of this model.

Whilst valuable information is obtained by field measurements to develop and validate the models, numerical models provide a useful tool to investigate unexplored sensitivity of the system to hypothetical scenarios (including for example larger arrays, different device characteristics, array configurations, and geographical settings, amongst others). The computational efficiency of the SWAN-SNL model has enabled a larger range of situations to be explored than might have been achieved by other models, which may better capture near-field effects. Development of phase-resolving wave models to investigate WEC effects is occurring (Rijnsdorp et al., 2017), and presents an advance on the model used here. However, these models are still computationally expensive and WEC device specific, precluding their use in a study such as that outlined here. In this study the analysis has been limited to how the wave properties are impacted by the presence of WEC arrays. This is primarily due to the wave field parameters being the only parameters that have been suitably validated with field data. An anticipated extension of this research is to investigate the effects of WEC array deployment on other morpho-hydro-dynamic factors, such as circulation, sea-bed evolution, and/or ecological consequences. The wave model and consequent results developed in this study are able to support a range of numerical models to investigate these other processes. For example, XBeach and Delft 3D are two models which could be implemented to investigate the morphological changes that might result from WEC array deployment. Suitable field-based validation of these models for these applications is required before their wide application.

The computational efficiency of SWAN-SNL has allowed us to explore many scenarios. However the number of possible scenarios is infinite. Where possible the sensitivity of wave climate was explored in detail, but in many cases (variables) we have only captured two alternative cases for bathymetric profile and array size to provide a comparison. This study aims to provide sufficient guidance as to the likely impact zones for proposed WEC deployments, to inform the design of a more rigorous set of simulations to be undertaken, which more fully capture the specific attributes of the planned deployment.

Results of our simulations would suggest that an array with many small capacity WECs will have less intense near-field impact than the same nameplate capacity array with fewer large capacity WECs. However, the SNL-SWAN model has severe limitations in that it does not account for relevant processes in this near-field region (e.g., diffraction or the radiated field generated by the WEC). Thus our confidence in these near-field responses is limited, and recommendations on array configurations to minimise near-field effects is best left to future study. These processes are less relevant for the mid-field effects, for which recommendations are given.

Field measurements of the effects of WEC deployment on the surrounding wave field have identified changes to the spectral characteristics of the wave field (Contardo et al., 2017). Simulation of these effects in the SWAN-SNL model required focussed efforts to ensure the frequency dependent transmission of energy through the WEC (array) was precise to adequately reproduce the observed spectral response. However the measured/modelled change in bulk wave parameters was well simulated without such precision (Contardo et al., 2017). The intent of this study is to provide preliminary guidance on the potential extent of impacts only, and consequently we consider only the changes in bulk wave parameters. It is expected that if notable changes in bulk wave parameters are predicted from this study, a more detailed study investigating the spectral wave response for the proposed deployment must follow.

The limitations of the wave model together with the use of idealised simulations to develop the generic tools necessarily limits its application to providing preliminary assessments and broad guidance of the impact of wave arrays. These preliminary assessments may inform the design of more detailed modelling assessments that account for the specific attributes of the devices and the local environment under investigation. The assessments may also be used to inform monitoring of the identified impacts by providing guidance of the most suitable locations for deployment of instrumentation. Factors such as the wave environment, the wave energy devices, their arrangement in arrays and the total power output have all been considered in developing a quantitative impact equation. The purpose of the equation is to provide preliminary guidance of the extent of potential physical impacts of proposed wave energy installations. Given the idealised nature of the experiments undertaken and the generalisation of the findings into a single impact equation, the guidance provided should be considered to be approximate at best, potentially providing the broad requirements for more detailed modelling in the specific coastal environment under consideration.

Broad findings about how WECs can influence the wave climate in the mid- to far-field down-wave of the WEC array were also identified from the idealised simulations. These are summarised as follows:

- 1) The impact of WEC arrays containing many devices with lower power ratings will have less intense (point-source) impact on the near to mid field than fewer devices that extract larger amounts of power. Maximising power extraction for a single device will therefore have a larger impact on the near- to mid-field environment.
- 2) Proximity of an array of WECs to the coast will increase impacts on the breaking zone. Analysis presented here of the coastal impacts of energy removed due to WECs is limited. However, simulations show significant changes in the radiation stress force associated with the predicted energy reductions could be expected. Thus we conclude that if the cross-shore impacted distance

in the wave field (e.g., in H_s) intersects the wave breaking depth, then the equilibrium state of the coastal zone will likely be disturbed leading to changes in coastal properties (e.g., shoreline position). This may be considered a positive or negative effect – for example, in some cases, a WEC array might be deployed as a coastal management solution. The recommendation from this study is if the estimated cross-shore impact distance intersects the 10-m depth contour, a more rigorous impacts study is required for the coastal zone.

- 3) A directional wave climate that is more widely distributed (e.g. Sydney) will have a less focussed impact on the coastline than a narrow directional wave climate.

Several hypothetical situations were provided to illustrate the potential application of the impact equation. It is noted that the determination of what is considered to be a damaging impact in terms of a threshold change to the present wave climatology is beyond the scope of the present study since it will be informed by the particular attributes and values of the coastal environment under consideration (e.g. the sensitivity of a particular species to changing environmental conditions).

References

- Abanades, J., D. Greaves, and G. Iglesias, 2015a: Coastal defence using wave farms: The role of farm-to-coast distance. *Renewable Energy*, **75**, 572-582.
- Abanades, J., D. Greaves, and G. Iglesias, 2015b: Wave farm impact on beach modal state. *Marine Geology*, **361**, 126-135.
- Alexandre, A., T. Stallard, and P. Stansby. Transformation of wave spectra across a line of wave devices. in Proceedings of the 8th European Wave and Tidal Energy Conference, Uppsala, Sweden. 2009
- Ashton, I., J. Saulnier, and G. Smith, 2013: Spatial variability of ocean waves, from in-situ measurements. *Ocean Engineering*, **57**, 83-98.
- Babarit, A., J. Hals, M.J. Muliawan, A. Kurniawan, T. Moan, and J. Krokstad, 2012: Numerical benchmarking study of a selection of wave energy converters. *Renewable Energy*, **41**, 44-63.
- Black, C., Analysis of waves in the near-field of wave energy converter arrays through image processing. *MSc Thesis, Oregon State University*. 2014. Available from: https://ir.library.oregonstate.edu/concern/graduate_thesis_or_dissertations/3f462881f
- Camus, P., F.J. Mendez, R. Medina and A. S. Cofino, 2011: Analysis of clustering and selection algorithms for the study of multivariate wave climate. *Coastal Engineering*, **58**, 453-462.
- Government of Western Australia, 2010: Renewable Energy handbook, 73 pp. available from: https://www.finance.wa.gov.au/cms/uploadedFiles/Public_Uilities_Office/Businesses_and_Government/Planning_renewable_energy_projects/Renewable_Energy_Handbook_2010.pdf
- Government of Victoria, D. o. Environment, Land, Water and Planning, 2016: Guideline for Marine Energy Tenures on Crown Land, 14 pp.
- Chowdhury, S. and R. Manasseh, 2017: Behaviour of eigenmodes of an array of oscillating water column devices. *Wave Motion*, **74**, 56-72.
- Contardo, S., R. K. Hoeke, M. A. Hemer, and K. L. McInnes, 2017: Transformation of wave spectra by an array of Wave Energy Converters. *Submitted to Coastal Engineering*.
- Copping, A., and Coauthors, 2016: Annex IV 2016 State of the Science Report: Environmental Effects of Marine Renewable Energy Development Around the World., 200 pp.

- Durrant, T., Greenslade, M. Hemer and C. Trenham, 2014: A Global Hindcast Focussed on the Central and South Pacific. CAWCR Technical Report, 70.
- Falcão, A. F. d. O., 2010: Wave energy utilization: A review of the technologies. *Renewable and Sustainable Energy Reviews*, **14**, 899-918.
- Flocard, F., and R. K. Hoeke, 2017: Coastal protection through wave farms: feasibility assessment using numerical wave modeling and parametric study. *Coasts and Ports Conference*.
- Folley, M., and T. J. T. Whittaker, 2009: Analysis of the nearshore wave energy resource. *Renewable Energy*, **34**, 1709-1715.
- Haller, M.C., et al., Laboratory Observation of Waves in the Vicinity of WEC-Arrays. 2011, Oregon Wave Energy Trust.
- Hemer, M. A., Z. Stefan, T. Durrant, J. O. O’Grady, R. K. Hoeke, K. L. McInnes, and U. Rosebrock, 2016: A Revised Assessment of Australia’s National Wave Energy Resource. *Renewable Energy*
- Leary, D., and M. Esteban, 2009: Climate Change and Renewable Energy from the Ocean and Tides: Calming the Sea of Regulatory Uncertainty. *The International Journal of Marine and Coastal Law*, **24**, 617-651.
- Manasseh, R., K. L. McInnes, and M. A. Hemer, 2017a: Pioneering developments of marine renewable energy in Australia. *International Journal of Ocean and Climate Systems*, **8**, 50–67.
- Manasseh, R., S. A. Sannasiraj, K. L. McInnes, V. Sundar, and P. Jaliha, 2017b: Integration of wave energy and other marine renewable energy sources with the needs of coastal societies. *International Journal of Ocean and Climate Systems*, **8**, 1-18.
- McNatt, J.C., 2012: Wave field patterns generated by wave energy converters. *M.Oc.E. Thesis, Oregon State University* 2012. Available from:
https://ir.library.oregonstate.edu/concern/graduate_thesis_or_dissertations/s7526g43s
- O’Hagan, A-M., 2016: Consenting Processes for Ocean Energy: Update on Barriers and Recommendations. IEA Ocean Energy Systems. Available at: <https://www.ocean-energy-systems.org/documents/55868-report-consenting-processes-2016.pdf/>
- O’Boyle, L., B. Elsässer, and T. Whittaker, 2017: Experimental Measurement of Wave Field Variations around Wave Energy Converter Arrays. *Sustainability*, **9**, 16.
- Rijnsdorp, D.P., J. Hansen and R. Lowe, 2017: Improving predictions of the coastal impacts of wave farms using a phase-resolving wave model. *Proc. 17th European Wave and Tidal Energy Conference, 25-Aug – 1-Sep, 2017, Cork Ireland*.

- Ruehl, K., A. Porter, C. Chartrand, H. Smith, G. Chang and J. Roberts, 2015: Development, Verification and Application of the SNL-SWAN Open Source Wave Farm Code. In: *Proc. 11th European Wave and Tidal Energy Conference, 6-11 Sep, 2015, Nantes, France.*
- Shields, M. A., and Coauthors, 2011: Marine renewable energy: The ecological implications of altering the hydrodynamics of the marine environment. *Ocean & Coastal Management*, **54**, 2-9.
- Simas, T., and Coauthors, 2015: Review of consenting processes for ocean energy in selected European Union Member States. *International Journal of Marine Energy*, 9, 41-59.
- The SWAN Team, 2017. SWAN User Manual, Delft University of Technology, 135p. Available at: <http://swanmodel.sourceforge.net/download/zip/swanuse.pdf>
- Winship, B., A. Fleming, I. Penesis, M. Hemer and G. Macfarlane, 2017: Preliminary investigation on the use of tank wall reflections to model WEC array effects. *Ocean Engineering*. Submitted.
- Witt., M.J. and co-authors, 2011: Assessing wave energy effects on biodiversity: the Wave Hub experience. *Phil. Trans. Roy. Soc. A.*, 370 (1959), doi: 10.1098/rsta.2011.0265

Appendix A: Australian Wave Energy Resource and Developments

A.1 Wave Energy Resource in Australia

Australia's long southern-facing coastline gives rise to arguably the largest wave energy resource of any country in the world. A comprehensive assessment of wave-energy resource in Australia estimates the total wave-energy flux across the depths of 25, 50 and 200 m to be 1796, 2652 and 2730 TW h/year, respectively (Hemer et al., 2016). This available energy is an order of magnitude larger than the 248 TW h electricity generated in Australia in 2013–2014 (Department of Industry and Science, 2015), and indicates that the magnitude of the wave resource is not a constraint to its future uptake. The vast majority of this resource is available to the southern coastal region with 1455 TW h/year estimated at the 25-m depth contour (the depth around which many wave devices are presently being tested), from 29°S on the Western Australian coast to 148°E on the southern tip of Tasmania including western Victoria. By contrast, the wave-energy resource over northern Western Australia (north of 23.5°S) and Northern Territory at the 25-m contour is 61 TW h/year.

Wave variability is also an important consideration for wave-energy extraction. An assessment of wave variability at the 25-m isobath indicates that much of the southern, mid-latitude coastal region is also favourable because it displays relatively low variability in wave energy with respect to the total available wave energy. In other words, large waves are generally not much greater than the wave height at which most energy is received, and episodes of minimum wave heights and energy ($H_s < 1$ m) are relatively short-lived, typically exhibiting durations of less than a day and are relatively uncommon with typically >100 days between events. Conversely, in the tropical north, the lower available wave resource is also characterised by a larger ratio of large waves to mean wave height. This is due to the occurrence of tropical cyclones. This region also experiences periods of minimal wave energy that are more frequent and of longer duration (Hemer et al., 2016).

A.2 Wave Energy Development in Australia

Globally, a wide variety of WEC device designs are under development. Over the past 10 years, Australia has been the setting for a number of marine renewable energy developments. Using the internationally-accepted Technology Readiness Level system (e.g. Makin, 2009) in which the developing technology is rated from 1 (Basic principles observed and reported) to 9 (Actual system proven in environment), ocean trials in Australia have demonstrated technology at up to a TRL of 7 (System prototype demonstration in

environment). The locations of the various trials that have been undertaken in Australia are shown in Figure 1 and indicates that trials to date have occurred along the wave energy-rich coastlines of the southern half of the continent. Each of the devices that have been trialed have different conditions to which they are ideally suited, and can be deployed in a range of situations from on the shoreline, to near-shore water depths, and offshore in water depths exceeding 100 m.

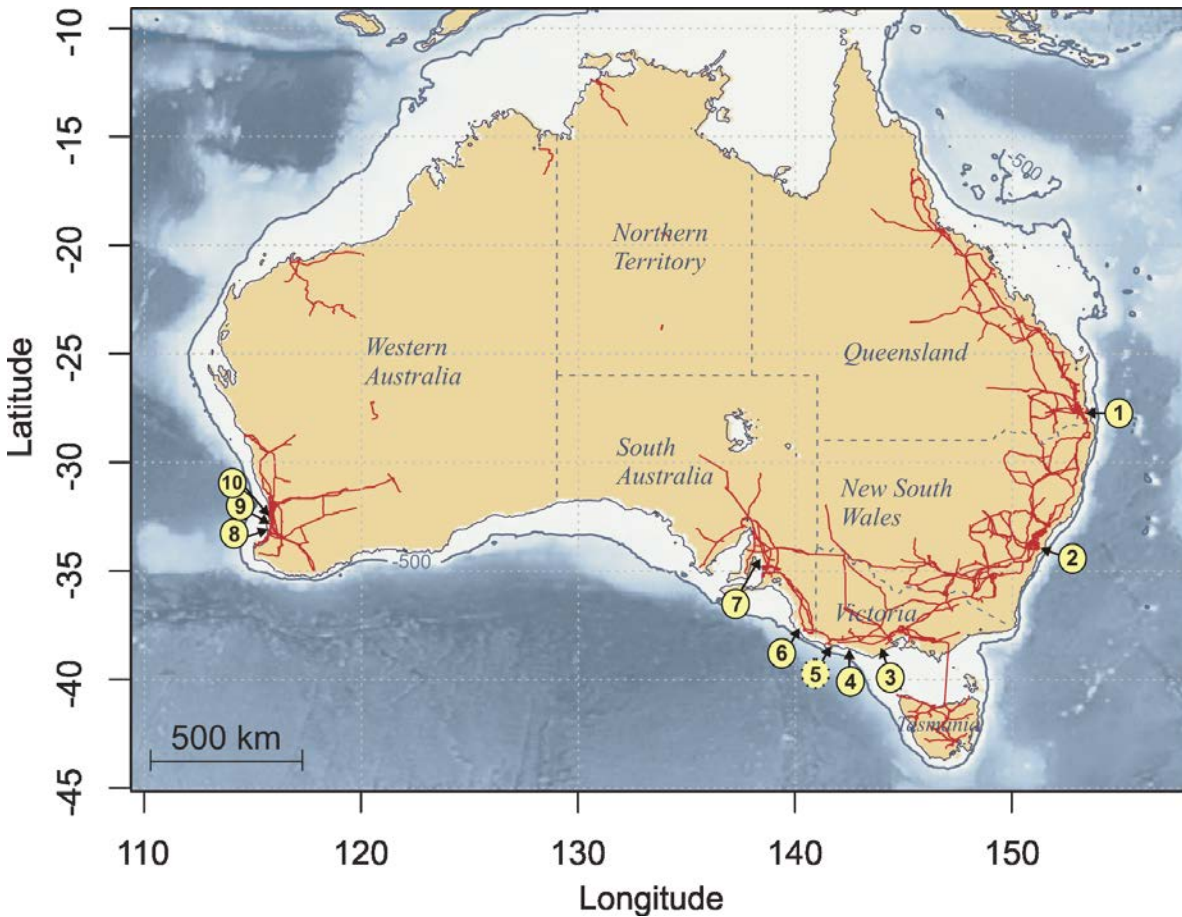


Figure A.1. Locations of marine-energy trials in Australia. Solid surrounded circles represent wave-energy trials, while symbols with dotted surrounds indicate locations where pre-trial feasibility assessments have been undertaken. Electricity transmission lines are shown in red. Further details are provided in Table 1. Adapted from Manasseh et al (2017).

WEC design is important since it determines the WECs suitability for different operating environments including the optimal depth of deployment, wave energy potential of the device and distance to shore. These considerations in turn determine the feasibility of the wave energy project.

Wave Energy Converter (WEC) technologies derive energy from the reciprocating motion of ocean waves, which can be harnessed in a variety of different ways (Falcao, 2010; Manasseh et al, 2017a) and accordingly

different classification systems have emerged for categorising the various device designs (Manasseh et al, 2017b). The first categorisation, referred to as the Directional Classification (DC) is based on the influence that the WEC has on the wave field. This classification describes devices as *point absorbers*, *attenuators* and *terminators*. The second classification system, referred to as the Morphological Classification (MC) divides devices according to their physical structure such as *oscillating water columns*, *heaving buoys*, *overtopping converters* and so on. A third proposed classification system described in Manasseh et al. (2016) refers to the physical operating principal (Operating Classification – OC) on which the device is designed. For example, devices may be classified as *point absorbing linear resonators*, *wavelength-tuned linear resonators* or *absorbers*. The OC classification also describes whether the basic operating principal is that of a pendulum (01) or a spring (02) and whether the device is large, medium or small in relation to the typical wavelength of the wave field it is deployed in. This latter classification therefore embeds more detail around the engineering aspects of the device than the DC classification.

The characteristics of the devices trialled around Australia as shown in Figure 1 are also summarised in Table A.1 in terms of the MC and OC classification systems. For a detailed history of these developments, the reader is referred to Manasseh et al. (2017a).

Table A.2 Summary of wave devices considered or trialed around Australia together with their various attributes according to the different available classification systems. Adapted from Manasseh et al (2016, 2017). MC: morphological classification; OC: operating principle classification; PALR: point-absorbing linear resonator; OWC: oscillating water column; WAB: wave activated body; WTLR: wavelength-tuned linear resonator; OTC: overtopping converter. Subscripts s, m and x denote short, medium and long devices, respectively. WTLR01); MC: OWC, floating.

	Location	Year	Company	Device type		Power rating	Operational depth
1	Gold Coast	2016	Wave Mill	OWC, floating	WTLR01	~ 3 kW	5-10 m
2	Port Kembla	2006	Oceanlinx	OWC, fixed	PALR01 _x	Up to 2.5 MW	~11 m
3	Lorne		Aquagen	WAB, heave	PALR02 _m	1.5 kW	~5 m
4	Port Fairy	2015	Biopower Systems	WAB rotation, fixed	PALR01 _m	250 kW	~5 m
5	Portland	-	Victorian Wave Partners Ocean Power	WAB, (two-body array)		19 MW (45 buoys)	
6	Port McDonnell	2014	Oceanlinx	OWC, fixed	PALR01 _x	1 MG	
7	Adelaide	2011	Waverider	WAB array	WTLR02	500 kW	
8	Bunbury		Protean	WAB, heave	PALR02 _m		
9	Garden Island	2014	Carnegie	WAB, heave	PALR02 _m	Up to 250 kW	24 m
10	Fremantle		Bombora	Non-resonating bladder	Absorber		

Appendix B: Planning and Legislative Considerations

The planning and development of wave energy projects requires approvals from authorities within different levels of government at different stages of the project cycle. Projects operating within 3 nautical miles offshore and the coastal high water mark fall under State Government controls whereas those operating beyond the 3 nautical model limit fall under Commonwealth controls. Shore cable connection of these offshore deployments will span State and Local Government waters, and are therefore subject to coinciding controls. Table 2 provides a summary of relevant state-based information.

Wave energy converter deployments typically target particular depths, with many designs targeted at depths of ~25-30 m. This targeted depth aims to capture the energy of the waves before it is lost through sea-bed friction processes. The 25-30 m depth contour often coincides closely with the 3 nm limit and so wave energy projects may require Commonwealth approvals, in addition to those required from Local and State Government associated with shore connections. Local and State Government processes differ by jurisdiction, with some regions having more mature process than others. Guidance and information on the processes required for obtaining approvals to conduct wave energy projects across Australia is provided below.

A wave energy project cycle typically consists of the following stages (Govt. WA, 2010);

- Preliminary evaluation;
- Feasibility study;
- Project design; and
- Implementation and operation.

The preliminary evaluation stage involves an exploration of options such as an assessment of the wave energy resource at potential sites of interest and a preliminary financial evaluation typically based on information from comparable projects and incorporating potential revenue streams such as Renewable Energy Certificates. Relevant information at this stage such as wave energy resource, proximity to the electricity grid, other marine resource users and so on can be obtained from the Australian Wave Energy

Atlas (AWavEA) (<http://nationalmap.gov.au/renewables/>). Other considerations are the selection of appropriate technology for the project, access to land, relevant approvals and access to the energy market.

The feasibility stage will involve a detailed assessment of the technical and economic viability of the project including potential barriers to the project. Relevant information at this stage includes a detailed project assessment including a site assessment that considers factors such as proximity to sensitive environmental areas and infrastructure access. Other factors to consider are local community issues, the intended uses of the energy produced, access to a workforce. A preliminary engineering assessment typically will consider capital costs and costs of supporting infrastructure, operation, electrical connection, revenue streams from energy and Renewable Energy Certificates (RECs), an environmental impact assessment and assessment of relevant legislation and policies. A timetable for implementation of the project should also be developed.

The project design phase involves finalising agreements and approvals such as a Power Purchase Agreements (PPA) and securing investment and funding from financiers. At this stage a Project Definition Document (PDD) is developed that provides detailed technical information, details of the PPA, environmental and planning approvals and investment information and support from government agencies. Following approval and sign-off of the PDD, the project can proceed to the implementation stage. This involves entering formal contractual arrangements with relevant entities, undertaking the detailed design, construction and commissioning of the project.

Table 3 State-based guidance material available to support the development of wave energy projects

State	Relevant Information	Comments
Victoria	Guideline for Marine Energy Tenures on Crown Land	Available from Victorian Department of Environment, Land, Water and Planning (nicola.waldron@delwp.vic.gov.au)
WA	Renewable Energy Handbook (2010)	available from https://www.finance.wa.gov.au/cms/index.aspx
NSW	NSW regulatory framework for marine energy deployments	Available from NSW Department of Industry (susan.shaw@industry.nsw.gov.au)
SA	General information on renewable energy including investors guide	http://www.renewablesa.sa.gov.au/

Appendix C: Characterising Wave Climates using MDA

The wave climates selected for assessment were based on Perth, Albany, Port Fairy and Sydney. To represent the nearshore wave climates of these four locations, a maximum dissimilarity (MDA) algorithm (Camus et al., 2011) was used to find a statistically representative subset of possible sea states in each location. The application of the MDA algorithm reduces the number of simulations needed to characterise a multiyear nearshore wave climate (both with and without WECs). The MDA algorithm selects a subset of size M representing wave climate states from a larger set of n -dimensional vectors of size N representing the entire wave climate at a location. It does so by successively finding the vector in N most dissimilar to those within M , removing the vector from N and adding it to M ; this requires selection of an initial vector to start the process (Kennard and Stone, 1969; Camus et al., 2010). As discussed by Camus et al. (2010 and 2011), depending on the size of M , MDA can be a highly efficient approach to reduce the number of sea states needed to characterise the nearshore wave climate, since each subset member can represent an actual sea state rather than some cluster-average and the subset covers the entire data space.

The N -member set used here is $X = \{CgE, Tp, \vartheta p\}$, i.e. hourly vectors of wave energy flux, peak period and peak direction, respectively, between years 1980 and 2014 ($N = 298057$). The MDA is initialised with the vector with the largest CgE value at each location; subsequent dissimilarity is calculated using the (normalised) Euclidean-circular (EC) distance and the MaxMin approach described in detail by Camus et al. (2010). Although MDA is not technically a clustering technique, points in the full set with the closest EC to each member of the subset can be considered a “cluster” allowing a probability to be assigned to each subset member. To illustrate, Figure A.1 shows an example of this using a simplified vector ($X = \{CgE, Tp\}$) and $M = 50$.

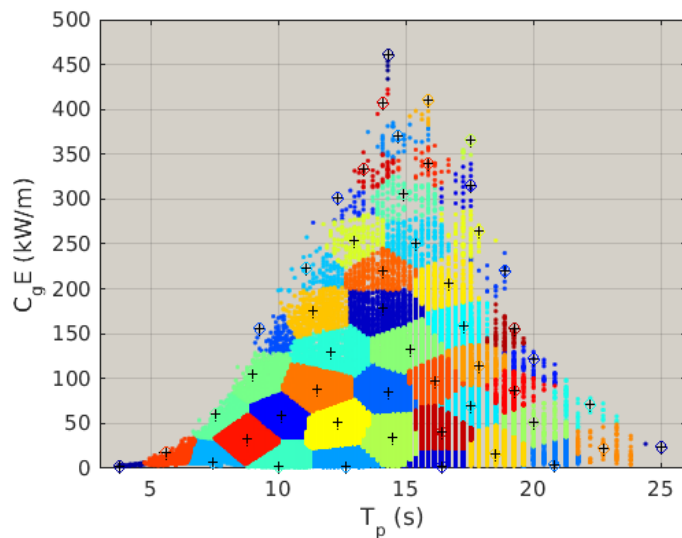


Figure C.1 an example of maximum dissimilarity (MDA) algorithm for a 50-member subset ($M=50$) of a larger set (N). The coloured dots indicate the simultaneous hourly CgE and T_p vectors for years 1980 to 2014 which compose N . Black crosses indicate members of M . The colour of the dots indicate the members of N that are closest (in EC distance) to respective member of N , creating a “cluster”.

To evaluate how well the M -subset compares to the full N -set (using $X = \{CgE, T_p, \vartheta p\}$), the empirical cumulative distributions for $M=100$, $M=500$ and $M=1000$ are compared at the four locations (Figure C.2). They show that while comparisons of all three values of M pass a two-tailed Kolmogorov–Smirnov (KS) test, the higher M values result in significantly reduced (improved) KS statistic and quantiles more closely matching the full N set (Table C.1).

Table C.1 CgE goodness of fit comparisons for each of the study locations: 50th and 98th percentiles (quantiles) of the 100, 500 and 1000 M member subsets and the N set, followed by the two-tailed Kolmogorov–Smirnov statistic (KSstat) comparing the empirical cumulative distribution functions (CDFs) of the M subsets with the N set. Percentile values are in kW/m.

	Perth			Albany			Port Fairy			Sydney		
	p50	p98	KSstat	p50	p98	KSstat	p50	p98	KSstat	p50	p98	KSstat
$M=100$	5.81	136.27	0.451	23.99	236.18	0.386	57.84	270.33	0.353	2.79	58.51	0.411
$M=500$	25.98	132.03	0.201	41.07	222.81	0.144	53.03	251.49	0.179	5.84	55.63	0.281
$M=1000$	20.85	134.97	0.129	44.97	223.81	0.099	48.78	251.38	0.092	8.30	56.20	0.183
N	20.60	134.10	-	44.10	220.80	-	48.00	249.40	-	7.80	54.80	-

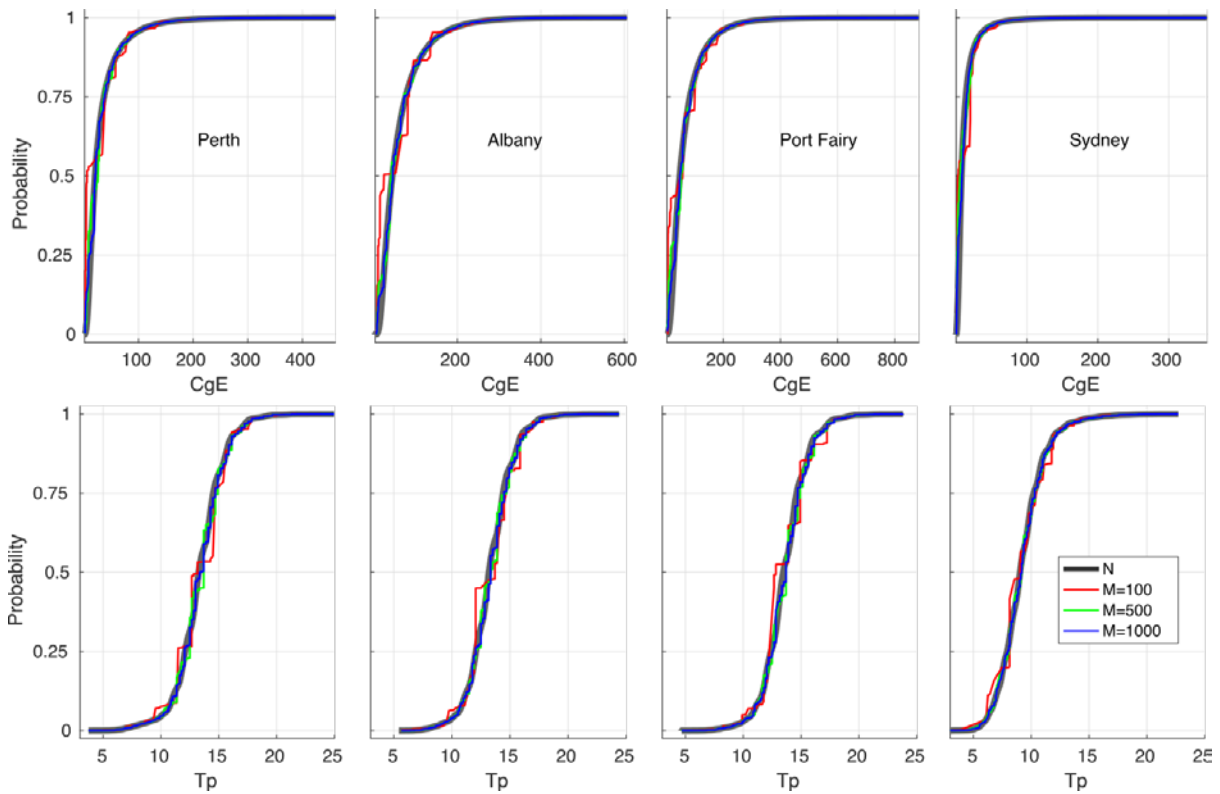


Figure C.2 Empirical cumulative distribution fits of the N set with the 100, 500 and 1000 M member subsets for each of the study sites. Top: CgE (units kW/m); bottom: Tp (units s).

Based on these results, the $M=500$ subset was selected as a good compromise between reproducing the statistics of the full N set and computational efficiency at all four wave climate locations (Perth, Albany, Port Fairy and Sydney) and were selected for analysis and use in the downscaling/WEC array comparison simulations in this study.

Appendix D: Nearshore Morphology

Two different bathymetric profiles were selected to investigate the effect of bed slope on the attenuation of the wave signal at the shoreline by WECs situated in 25 m of water. The profiles considered for the experiment were: 1) a steep profile where the 25 m depth contour was 2 km offshore, representative of an Australian east coast profile, and 2) a gentle profile where the 25m depth contour is 4 km offshore, representative of an Australian south or west coast profile (Figure 3). The commonly used Dean profile (RG Dean 1977 Equilibrium profile) was used to define the bathymetric height (z) and is given by the equation:

$$z = ax^b, \quad \text{Equation D.1}$$

where a is the dimensionless steepness scale parameter and b is the dimensionless shape exponent and x is the distance offshore. For both bathymetric profiles the shape parameter is set to the default $b = 2/3$. The scale parameter for the east coast profile was $a = -0.1$, and for the west and south coast profile $a = -0.1575$.

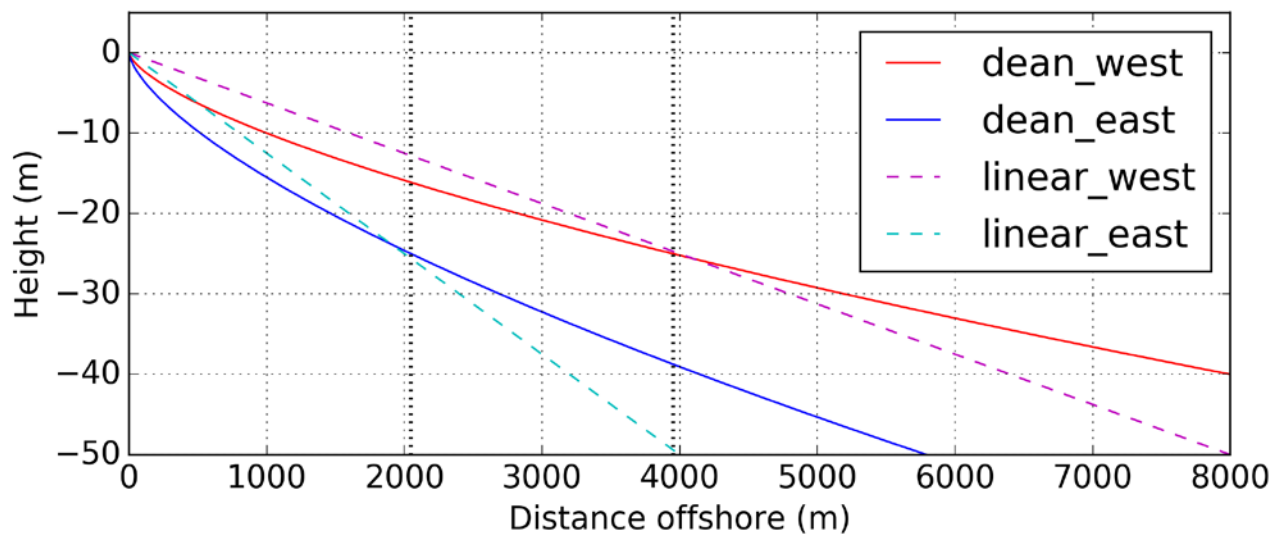


Figure D.1 Bathymetric profiles for idealised sensitivity experiments.

Appendix E: SNL-SWAN Model Configuration

The SNL-SWAN simulations were setup to represent an idealised nearshore environment with a straight shoreline, longshore uniform bathymetry as described in Section 3.5 and Appendix D. The physical domain setup and obstacle blocking by SNL-SWAN were outlined in Section 3. Here an example input file is provided; this illustrates that many of the model physics parameterisation such as wave breaking, bottom friction utilise default settings (e.g. see the SWAN user manual).

E.1 Example SNL-SWAN input file

```
PROJECT 'ARENA' 'GLs' $Perth B-OF 3 MW farm square row config on gentle profile
'Guidelines Sims'
SET NAUT
SET inrhog = 1
SET obcase = 1
MODE STAT TWOD
COORD CARTESIAN
CGRID REG 0 0 0 5970 11970 199 399 SECTOR 0 180 90 0.035 0.5 40
INPGRID BOTTOM REG 0 0 0 199 399 30 30
READINP BOTTOM -1 './../Bathymetry_PF1.bot' 3 1 FREE
$
BOUND SHAPESPEC JONSWAP 1 PEAK DSPR DEGREES
BOUNDSPEC SIDE E CON PAR 5.02 17.54 96.0 26.7
BOUNDSPEC SIDE N CON PAR 5.02 17.54 96.0 26.7
BOUNDSPEC SIDE S CON PAR 5.02 17.54 96.0 26.7
$
BREAKING
FRICTION
OFF QUADRUPL
OFF WCAPping
$
OBSTacle TRANSm 0.0 LINE 2007.0 6006.0 2007.0 5997.0
OBSTacle TRANSm 0.0 LINE 2007.0 6006.0 2016.0 6006.0
$
TABLE 'COMPGRID' NOHEAD 'SWANOUT.DAT' HSIG DIR RTP TRANSP FORCE UBOT DISSURF
COMPUTE
STOP
```

Appendix F: Impact zone analysis

SNL-SWAN gridded model output is stored in data arrays for the Control ($C_{i,j,k}$) and WEC-attenuated ($W_{i,j,k}$) simulations. The output is stored for the variables Hs , CgE , Uo and D_{surf} have the dimensions i in longshore $x = 1:200$, j in shore-perpendicular $y=1:400$ and k in MDA event= $1:500$. The change presented in this report as a result of including the array is defined for each variable as:

$$\Delta_{i,j,k} = (C_{i,j,k} - W_{i,j,k}) \quad \text{Equation F.1}$$

where $C_{i,j,k}$ is the output variable for the Control run and $W_{i,j,k}$ is the output variable for the WEC-attenuated run. The percentile climate grids are calculated looping through each spatial grid point (i,j), ordering the 500 values and picking off the value corresponding to the percentile value of the empirical cumulative distribution function of the probabilities for each of the 500 MDA values:

$$\dot{\Delta}_{i,j} = ECDF(\Delta_{i,j,k}, p) \quad \text{Equation F.2}$$

where $\dot{\Delta}_{i,j}$ is the percentile change in a wave field variable, p is the percentile, calculated for the 50th, 75th and 95th percentile climates. $\Delta_{i,j,k}$ in Equation F.2 is replaced with the control values $C_{i,j,k}$ to compute the baseline climate. Multiple spatial Impact metrics are applied to the percentile map conditions. The first impact metric is Area:

$$IA_{tot} = count[\dot{\Delta}_{i,j} \geq q] \cdot \Delta x \cdot \Delta y \quad \text{Equation F.3}$$

where IA_{tot} is the total area in the percentile map conditions impacted. The term q refers to an array of equally spaced values of the absolute change in a wave field variable for all values, or normalised change. E.g. For absolute changes in Hs , q range from 0.25m to 0.75 m in increments of 0.25 m. $\Delta x \cdot \Delta y$ are the grid spacing in the x and y direction.

The second impact variable is Impact distance in the shore-perpendicular direction:

$$ICS_{tot} = count [Lx_i \geq q] \cdot \Delta x \quad \text{Equation F.4}$$

$$Lx_i = columnmax[\dot{\Delta}_{i,j}]$$

where the columnmax function reduces the 2D percentile map conditions array to a 1D array in the shore-perpendicular direction Lx_i . The third impact variable is ILS, which is the total longshore distance of the impact of q .

$$ILS_{nsh} = count [Ly_i \geq q] \cdot \Delta y \quad \text{Equation F.5}$$

$$Ly_j = rowmax[\dot{\Delta}_{i,j}, Z_{i,j} \geq -10],$$

where the rowmax function reduces the 2D percentile map conditions array to a 1D array in the cross-longshore direction. $Lxtot,q$ is the total longshore distance impacted and $Lynsh,q$ is longshore extents (length width) of the impact of q .

The semi-empirical fitted to the SNL-SWAN impact data (IA_{tot} , ICS_{tot} and ILS_{nsh} in Equation F-3 to F-5) are based on a typical exponential decay formulation can be represented by the equation:

$$I(\Delta, F_{absorbed}) = a \cdot \exp(b \cdot \Delta \cdot F_{absorbed}^{-c}) + d, \quad \text{Equation F.6}$$

where the equation can be rearranged to solve for what a change will be for a impact spatial metric I (IA, ICS, ILS). The amount of power absorbed by the WEC array $F_{absorbed}$ is calculated with Equation 4. The coefficients a , b , c and d are the fitted parameters. The coefficients are different for each sensitivity, and are provided in Appendix G. A least squares optimiser was used to find the parameters a , b , c and d by minimising the difference between each of the SNL-SWAN impact data (Equation F-3 to F-5), and Equation F.6 with the corresponding impact change ($\Delta = q$) and power absorbed by the WEC array $F_{absorbed}$. Equation F.6 can also be rearranged algebraically to find the impact-change (Δ) for a selected impact spatial metric (IA, ICS, ILS):

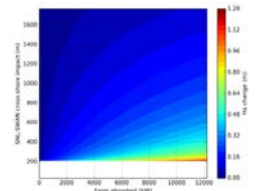
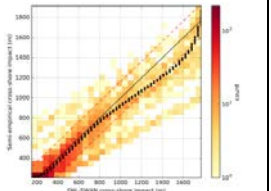
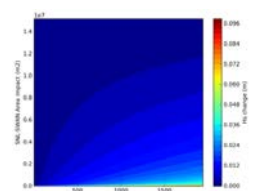
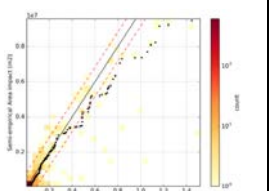
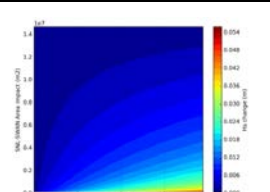
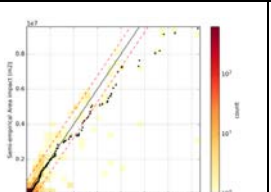
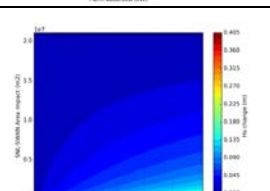
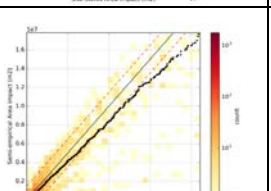
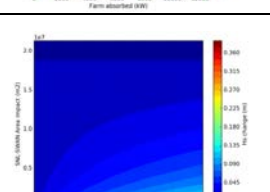
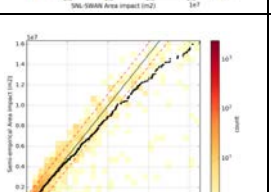
$$\Delta(I, F_{absorbed}) = \frac{F_{absorbed}^c}{b} \log\left(\frac{I - d}{a}\right) \quad \text{Equation F.7}$$

Appendix G: Empirical Equation Parameters.

Using the formulation of semi-empirical equations presented in Appendix F, a different set of coefficients are provided for a range of considerations including different variables, spatial metrics and bathymetric profiles and configurations. These sets of coefficients are presented here. We recommend the equations only be used where equation inputs are within the bounds of the lookup table(s).

Variable	Spatial impact / units	Profile	Farm Size	Row config	lookup plot	Model fit plot	a	b	c	d	RMSE
Hs	cross-shore / m	Gentle	3MW	two			4086.5	-	0.72	197.63	294.69
Hs	cross-shore / m	Gentle	3MW	square			3879.84	-	0.69	193.19	275.76

Hs	cross-shore / m	Gentle	20MW	two			4030.35	2430.42	0.6	250.56	279.64
Hs	cross-shore / m	Gentle	20MW	square			4126.18	4292.77	0.67	248.49	219.37
Hs	cross-shore / m	Steep	3MW	two			2391.14	5102.81	0.71	176.98	147.1
Hs	cross-shore / m	Steep	3MW	square			2462.59	4362.58	0.69	173.05	129.28
Hs	cross-shore / m	Steep	20MW	two			2003.17	1378.23	0.6	193.38	191.64

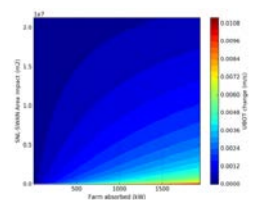
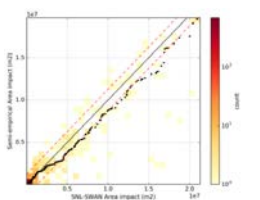
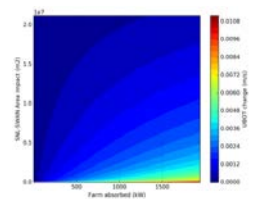
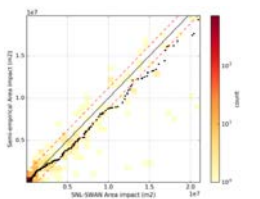
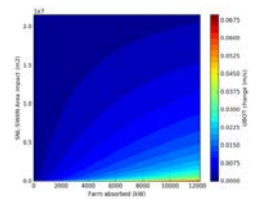
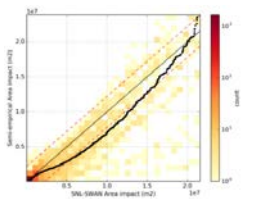
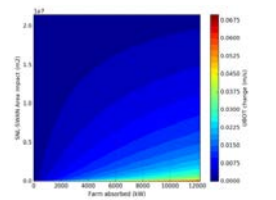
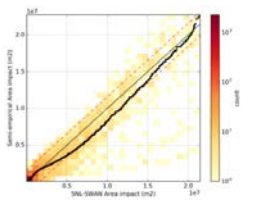
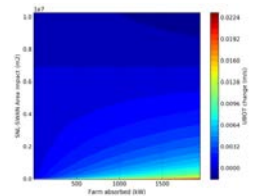
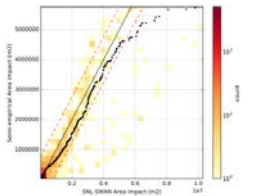
Hs	cross-shore / m	Steep	20MW	square			2473.58	2794.04	0.67	206.65	164.76
Hs	Area / m ²	Gentle	3MW	two			15872487	22526.2	0.71	50195.19	824894.8
Hs	Area / m ²	Gentle	3MW	square			15934160	24540.9	0.72	49467.65	749693.7
Hs	Area / m ²	Gentle	20MW	two			20548699	17928.7	0.72	63855.95	1482471
Hs	Area / m ²	Gentle	20MW	square			18738867	13665.5	0.69	65274.47	1130873

CgE	cross-shore / m	Gentle	3MW	two			4055.89	4145.82	1.17	191.24	306.75
CgE	cross-shore / m	Gentle	3MW	square			3905.95	3644.92	1.16	187.18	295.28
CgE	cross-shore / m	Gentle	20MW	two			4146.68	6801.25	1.13	281.78	256.63
CgE	cross-shore / m	Gentle	20MW	square			4081.12	-7098.7	1.16	234.71	189.87
CgE	cross-shore / m	Steep	3MW	two			2244.9	3322.57	1.2	172.44	147.81

CgE	cross-shore / m	Steep	3MW	square			2267.83	-2825.1	1.18	166.44	135.79
CgE	cross-shore / m	Steep	20MW	two			1830.93	3484.45	1.15	199.19	184.77
CgE	Area / m ²	Gentle	3MW	two			12263078	9239.34	1.15	47154.35	308391.2
CgE	Area / m ²	Gentle	3MW	square			12304141	10304.2	1.16	46618.2	295753.9
CgE	Area / m ²	Gentle	20MW	two			17759139	-36934	1.24	59796.8	865754.8

CgE	Area / m ²	Gentle	20MW	square			15461265	30663.6	1.23	63949.48	678611.2
CgE	Area / m ²	Steep	3MW	two			3621754	6078.27	1.17	33063.05	189615.1
CgE	Area / m ²	Steep	3MW	square			3648925	6926.67	1.18	34006.4	181443.7
UBOT	cross-shore / m	Gentle	3MW	two			4530.6	55390.8	0.73	189.56	363.65
Uo	cross-shore / m	Gentle	3MW	square			4101.52	41586.8	0.7	179.77	340.77

Uo	cross-shore / m	Gentle	20MW	two			5878.82	49674.6	0.72	281.76	412
Uo	cross-shore / m	Gentle	20MW	square			6456.28	62710.3	0.75	271.31	313.05
Uo	cross-shore / m	Steep	3MW	two			2902.4	42598.1	0.76	170.7	221.74
Uo	cross-shore / m	Steep	3MW	square			3272.82	38581.9	0.74	169.02	196.6
Uo	cross-shore / m	Steep	20MW	two			1440.01	68877.6	0.9	169.88	363.21

Uo	Area / m ²	Gentle	3MW	two			29056821	-140426	0.71	46577.66	1261490
Uo	Area / m ²	Gentle	3MW	square			29556112	-150314	0.72	45936.41	1203347
Uo	Area / m ²	Gentle	20MW	two			27492554	-161647	0.77	62660.32	2205660
Uo	Area / m ²	Gentle	20MW	square			25989123	-107715	0.73	59376.15	1566526
Uo	Area / m ²	Steep	3MW	two			6904719	69902.9	0.72	27290.22	757487.8

Uo	Area / m ²	Steep	3MW	square			6967548	74062.9	0.72	26563.53	734241.4
Uo	longshore / m	Gentle	3MW	two			30246.77	-84294	0.54	15.58	2190.78
Uo	longshore / m	Gentle	3MW	square			30656.82	85896.4	0.54	15.2	2086.74
Uo	longshore / m	Gentle	20MW	two			12798.47	15814.6	0.48	-139.19	2629.56
Uo	longshore / m	Gentle	20MW	square			12550.95	26412.7	0.54	-115.8	2379.72

Uo	longshore / m	Steep	3MW	two			7687.66	35194.3	0.57	-16.87	1345.87
Uo	longshore / m	Steep	3MW	square			7766.8	39704.7	0.58	-16.88	1325.15
Uo	longshore / m	Steep	20MW	two			5556.65	8233.07	0.52	30.59	1478.47
Uo	longshore / m	Steep	20MW	square			5525.58	12638.4	0.56	1.62	1319.2
Dsurf	longshore / m	Gentle	3MW	two			17796.51	4750.23	0.92	22.5	1151.19

Dsurf	longshore / m	Gentle	3MW	square			19277.57	5997.38	0.94	23.58	1181.72
DISSURF	longshore / m	Steep	3MW	two			6186.47	1324.87	0.95	5.29	933.26
Dsurf	longshore / m	Steep	3MW	square			6290.55	1554.08	0.97	6.38	910.7

Appendix H: Supplementary plots.

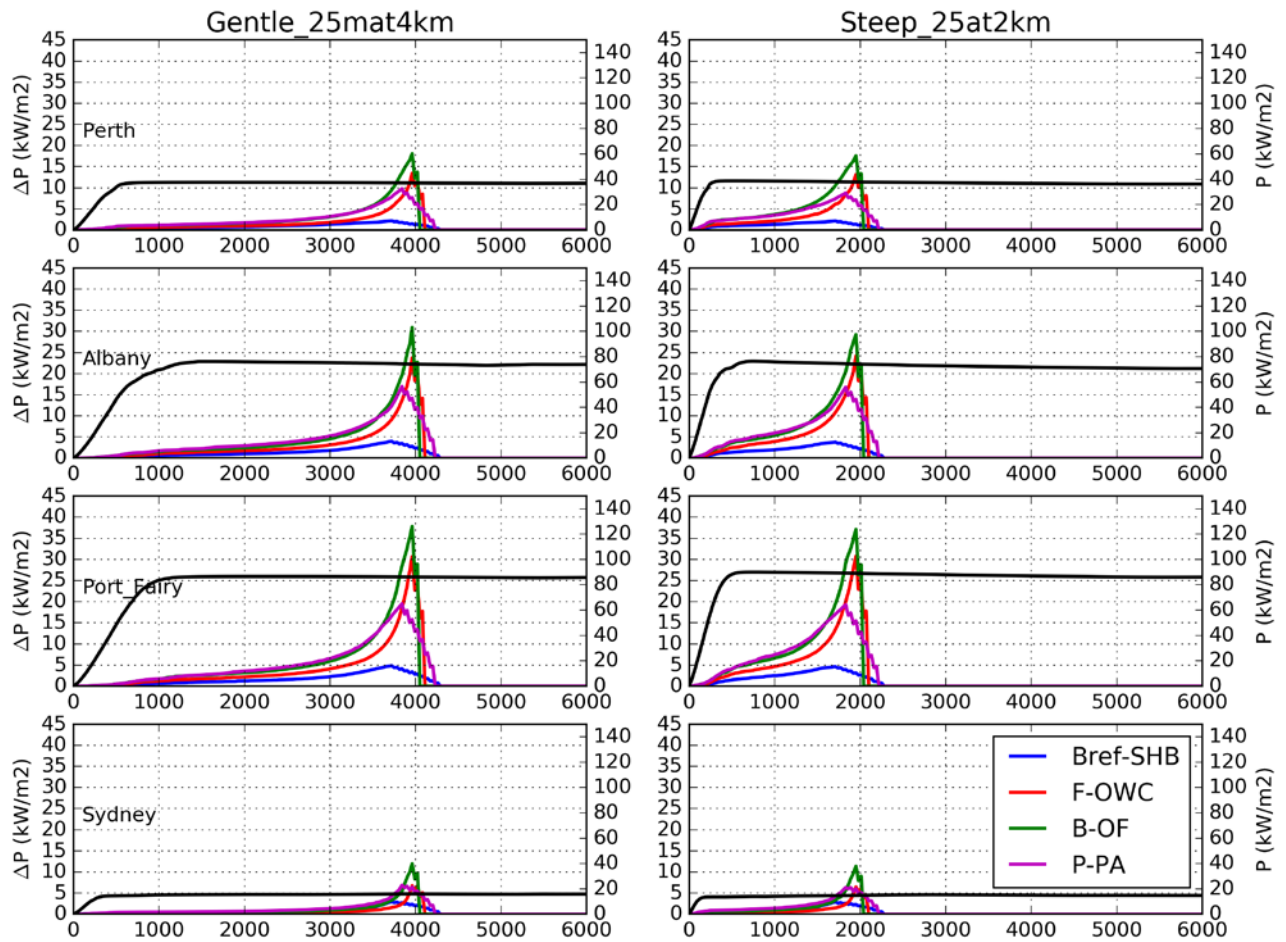


Figure I-1 *CgE* (labelled on the y-axis as *P*) shore-perpendicular transects of the change in 75th percentile climate. For the 20 MW square array configuration.

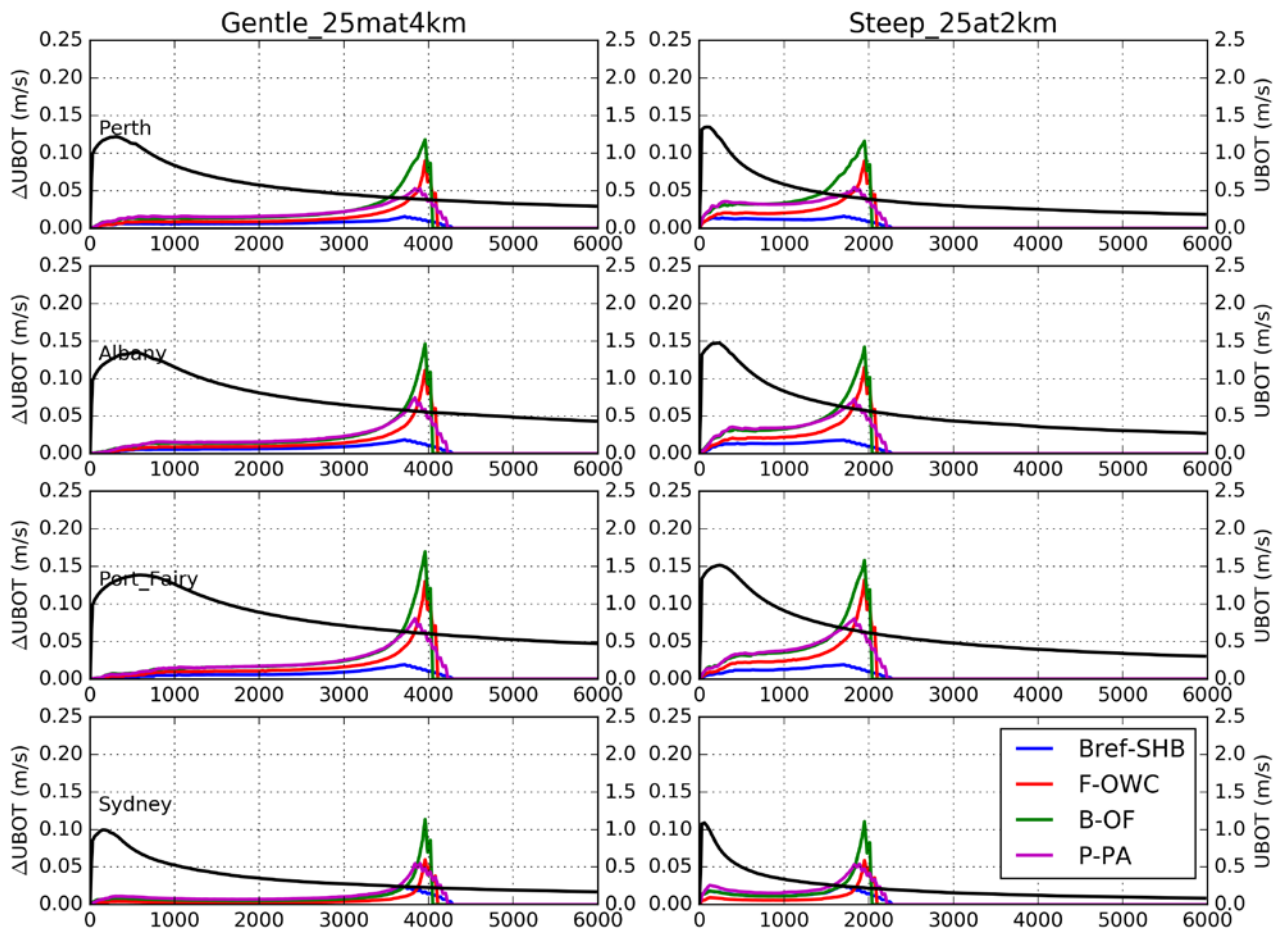


Figure I-2 U_o Shore-perpendicular transects of the change in 75th percentile climate. For the 20 MW square array configuration.

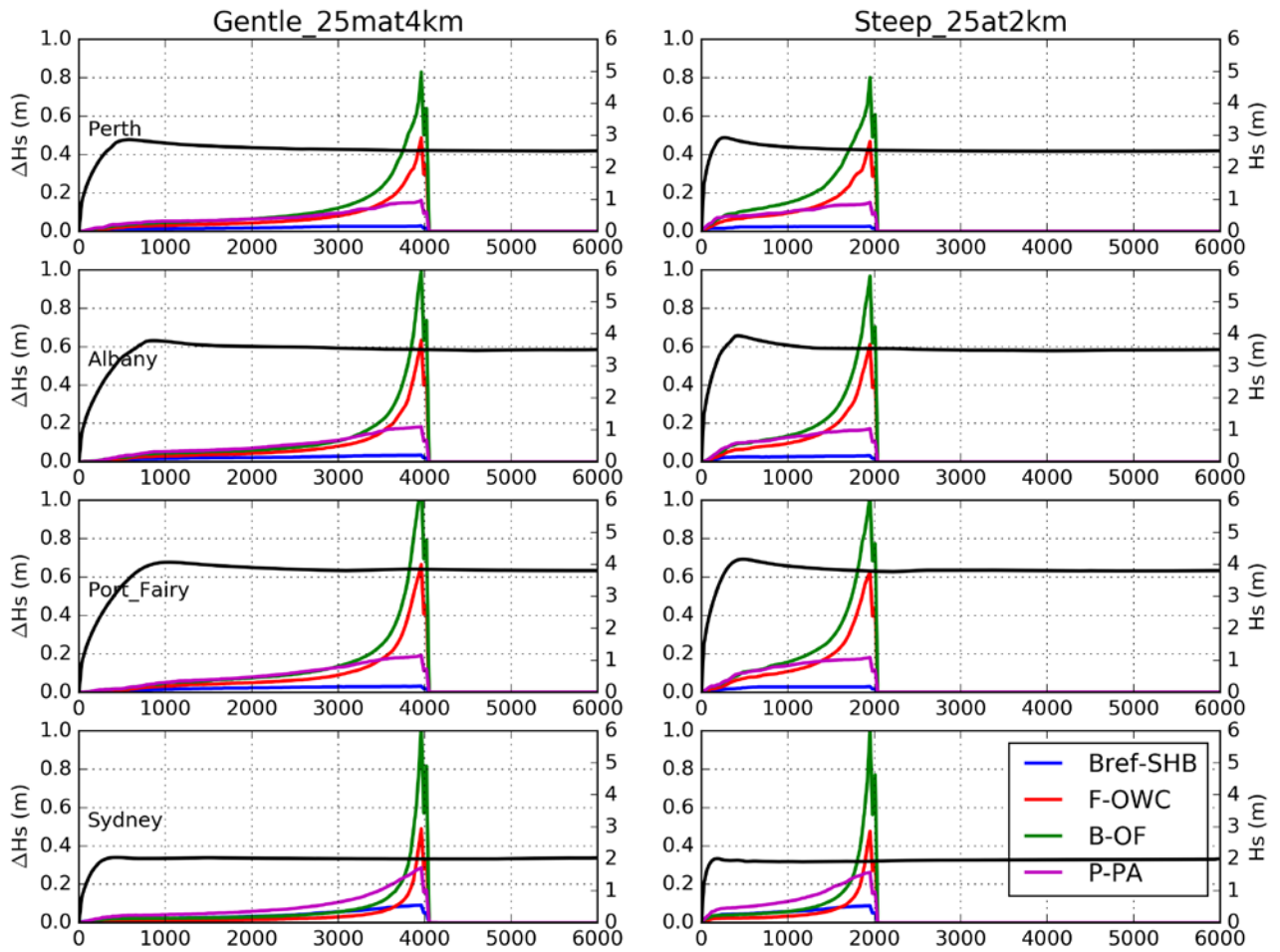


Figure I-3 H_s Shore-perpendicular transects of the change in 75th percentile climate. For the 20 MW two row array configuration.

CONTACT US

t 1300 363 400

+61 3 9545 2176

e enquiries@csiro.au

w www.csiro.au

At CSIRO we shape the future

We do this by using science to solve real issues. Our research makes a difference to industry, people and the planet.

As Australia's national science agency we've been pushing the edge of what's possible for over 85 years. Today we have more than 5,000 talented people working out of 50 - plus centres in Australia and internationally. Our people work closely with industry and communities to leave a lasting legacy. Collectively, our innovation and excellence places us in the top ten applied research agencies in the world.

WE ASK, WE SEEK AND WE SOLVE

For further information

Oceans and Atmosphere

Kathleen McInnes

t +61 03 9239 4569

e Kathleen.McInnes@csiro.au

w <http://www.cmar.csiro.au/sealevel/>